

**DOKUZ EYLÜL UNIVERSITY  
GRADUATE SCHOOL OF NATURAL AND APPLIED  
SCIENCES**

**DESIGN IMPROVEMENT OF RADIAL FANS ON  
DOMESTIC REFRIGERATORS BY NUMERICAL  
AND EXPERIMENTAL METHODS**

**by  
Enes GÖNENLİOĞLU**

**March, 2014  
İZMİR**

**DESIGN IMPROVEMENT OF RADIAL FANS ON  
DOMESTIC REFRIGERATORS BY NUMERICAL  
AND EXPERIMENTAL METHODS**

**A Thesis Submitted to the  
Graduate School of Natural and Applied Sciences of  
Dokuz Eylül University  
In Partial Fulfillment of the Requirements for the Degree of Master  
of Science in Mechanical Engineering, Energy Program**

**by  
Enes GÖNENLİOĞLU**

**March, 2014  
İZMİR**

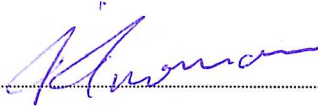
## M.Sc THESIS EXAMINATION RESULT FORM

We have read the thesis entitled “**DESIGN IMPROVEMENT OF RADIAL FANS ON DOMESTIC REFRIGERATORS BY NUMERICAL AND EXPERIMENTAL METHODS**” completed by **ENES GÖNENLİOĞLU** under supervision of **PROF. DR. DİLEK KUMLUTAŞ** and we certify that in our opinion it is fully adequate, in scope and in quality, as a thesis for the degree of Master of Science.



Prof. Dr. Dilek KUMLUTAŞ

Supervisor



Prof. Dr. İsmail Hakkı Tavman

(Jury Member)



Yrd. Doç. Dr. M. Turhan ÇOBAN

(Jury Member)



Prof. Dr. Ayşe OKUR

Director

Graduate School of Natural and Applied Sciences

## ACKNOWLEDGEMENTS

First of all, I would like to thank my supervisor, Assoc. Prof. Dr. Dilek KUMLUTAŐ, for her incomparable knowledge and moral support, valuable advises and guidance throughout this thesis study.

I also wish to express my gratitude to Assist. Özgün ÖZER at Department of Mechanical Engineering Energy program for their patience and help.

Finally, I would like to gratefully thanks to my family for their endless encouragement, patience and valuable support in every part of my life.

Enes GÖNENLİOĐLU

# **DESIGN IMPROVEMENT OF RADIAL FANS ON DOMESTIC REFRIGERATORS BY NUMERICAL AND EXPERIMENTAL METHODS**

## **ABSTRACT**

The aim of this study is to improve the flow characteristic at the exit region of a radial fan that is mounted on domestic refrigerators, which are used short term preservation of foodstuff in the home according to International Standards. For this purposes Particular Image Velocimetry (PIV) method was carried out on the fan and Computational Fluid Dynamics (CFD) method was used to validate the experimental results in order to determine the flow characteristic at the exit region of radial fan. After determination of natural flow direction by using the experimental and numerical investigations, a parametric study was implemented to optimize the flow direction at the exit region of the radial fan. The success of this study is to provide approximately equal velocity values and linear flow directions throughout the exit region of radial fans' duct. This developments' goal is not only implementation the homogeneous air distribution inside the refrigerator compartments but also increase the forced convection on the evaporators that is directly effected the cooling performance of the related volumes.

**Keywords:** Domestic refrigerators, radial fan, computational fluids dynamics, particular image velocimetry.

# EV TİPİ BUZDOLAPLARINDA KULLANILAN RADYAL FANIN SAYISAL VE DENEYSEL METOTLARLA TASARIMININ İYİLEŞTİRİLMESİ

## ÖZ

Bu çalışmanın amacı uluslararası standartlara uygun olacak şekilde gıdaların kısa süreli saklanması amacıyla evlerde kullanılan buzdolaplarına ait bir radyal fanın çıkış bölgesindeki akış karakteristiğinin geliştirilmesidir. Bu amaçla fanın hava çıkış bölgesindeki akış karakteristiği deneysel olarak Parçacık Görüntülemeli Hız Ölçümü (PGHÖ) yöntemiyle belirlenmiş, Hesaplamalı Akışkanlar Dinamiği (HAD) yöntemiyle de doğrulanmıştır. Deneysel ve sayısal çalışmalarla akışın yönünün belirlenmesinden sonra akış profilinin optimize edilmesi amacıyla parametrik çalışma yapılmıştır. Fanın çıkış ağızı boyunca yaklaşık olarak eşit hız değerlerinde ve doğrusal bir yönde akış karakteristiği sağlamak bu çalışmanın başarısıdır. Bu geliştirmelerin hedefi sadece buzdolaplarındaki bölmelerde homojen hava akışını sağlamak değil, aynı zamanda fanın bulunduğu bölmedeki soğutma performansını direk etkileyen evaporatörden olan zorlanmış taşınımı arttırmaktır.

**Anahtar kelimeler:** Ev tipi buzdolapları, radyal fan, hesaplamalı akışkanlar dinamiği, parçacık görüntülemeli hız ölçümü.

## CONTENTS

	<b>Page</b>
M.Sc THESIS EXAMINATION RESULT FORM.....	<b>ii</b>
ACKNOWLEDGEMENTS .....	<b>iii</b>
ABSTRACT.....	<b>iv</b>
ÖZ .....	<b>v</b>
LIST OF FIGURES .....	<b>viii</b>
LIST OF TABLES .....	<b>x</b>
<b>CHAPTER ONE - INTRODUCTION .....</b>	<b>1</b>
1.1 Literature Survey.....	3
<b>CHAPTER TWO - REFRIGERATORS .....</b>	<b>6</b>
1.1 History of Refrigerators Development .....	6
1.2 Domestic Refrigerating System Basics and Theories .....	8
1.2.1 The Ideal Vapor-Compression Refrigeration Cycle .....	9
1.2.2 Actual Vapor-Compression Refrigeration Cycle.....	13
1.3 Heat Transfer Mechanisms.....	15
1.3.1 Physical Mechanism of Convection .....	20
1.3.1.1 Nusselt Number.....	22
1.3.1.2 Prandtl Number .....	22
1.3.1.3 Reynolds Number.....	23
1.3.1.4 Grashof Number.....	24
1.3.1.5 Rayleigh Number .....	24
2.4 Domestic Refrigerators.....	25
2.4.1 Compressor .....	26
2.4.2 Condenser .....	29
2.4.3 Evaporator.....	32
2.4.4 Capillary Tube (Expansion Valve) .....	34
2.4.5 Refrigerants.....	35

<b>CHAPTER THREE - FAN.....</b>	<b>37</b>
3.1 Types of Fans. ....	39
3.1.1 Backward Curved Blades.....	40
3.2 Centrifugal Fan Mechanism. ....	41
<b>CHAPTER FOUR - EXPERIMENTAL STUDY .....</b>	<b>47</b>
4.1 Methodology of Particle Image Velocimetry (PIV).....	47
4.1.1 Equipment and Apparatus of PIV .....	48
4.1.1.1 Seeding Particles .....	49
4.1.1.2 Cameras and Lenses.....	50
4.1.1.3 Laser and Optics.....	51
4.1.1.4 Synchronizer .....	51
4.1.1.5 Analysis .....	51
4.1.2 Stereoscopic PIV Setup .....	52
4.2 Results .....	53
4.2.1 Full Model Experiment.....	53
<b>CHAPTER FIVE - NUMERICAL STUDY.....</b>	<b>59</b>
5.1 Methodology .....	59
5.2 Validation & Results .....	63
5.3 Parametric Study .....	65
<b>CHAPTER SIX - CONCLUSIONS.....</b>	<b>70</b>
<b>REFERENCES.....</b>	<b>71</b>



## LIST OF FIGURES

	<b>Page</b>
Figure 1.1 Cooling systems on domestic refrigerators.....	2
Figure 2.1 Schematic T-s diagram for the ideal vapor-compression refrigeration cycle .....	10
Figure 2.2 An ordinary household refrigerator .....	11
Figure 2.3 The P-h diagram of an ideal vapor-compression refrigeration cycle .....	12
Figure 2.4 Schematic and T-s diagram for the actual vapor-compression refrigeration cycle .....	14
Figure 2.5 Heat conduction through a large plane wall of thickness $\Delta x$ and area A .	16
Figure 2.6 Heat transfer from a hot surface to air by convection .....	17
Figure 2.7 Blackbody radiation represents the maximum amount of radiation that can be emitted from a surface at a specified temperature.....	19
Figure 2.8 A fluid flowing over a stationary surface comes to a complete stop at the surface because of the no-slip condition .....	21
Figure 2.9 The development of a boundary layer on a surface is due to the no-slip condition.....	23
Figure 2.10 Refrigeration circuit.....	26
Figure 2.11 A typical hermetic compressor .....	28
Figure 2.12 New, high-efficient compact coil air-cooled condensing units using hermetic compressors.....	29
Figure 2.13 Schematic of a natural draft condenser.....	30
Figure 2.14 Forced convection, plate fin–and-tube type condenser .....	31
Figure 2.15 Cycle defrost evaporator.....	33
Figure 2.16 Frost-free evaporator .....	34
Figure 2.17 Capillary tube.....	35
Figure 3.1 The five main fan types .....	37
Figure 3.2 Types of fan impellers_1 .....	39
Figure 3.3 Types of fan impellers_2 .....	40
Figure 3.4 Impeller with backward-curved blades and other details .....	43
Figure 3.5 Percentage decrease of density of moist air with decreasing temperature	45

Figure 3.6 Velocity triangles for backward-curved blades .....	45
Figure 3.7 $c_2u$ divided by $u_2$ plotted against $\alpha_2$ .....	46
Figure 4.1 Experimental arrangement of PIV in a wind tunnel .....	48
Figure 4.2 Densities of particle distribution.....	49
Figure 4.3 The schematic of lens and its focal plane .....	50
Figure 4.4 Schematic view of PIV set up components. ....	52
Figure 4.5 Calibration target and cameras .....	53
Figure 4.6 Lateral planes.....	54
Figure 4.7 Instantaneous SPIV results on investigation plane 04-05.....	55
Figure 4.8 Instantaneous SPIV results on investigation plane 07-09.....	55
Figure 4.9 Instantaneous SPIV results on investigation plane 11-17.....	56
Figure 4.10 Average three dimensional velocity distribution at the boundary region on investigation plane 1-2. ....	57
Figure 4.11 Average three dimensional velocity distribution at the boundary region on investigation plane 3-4. ....	57
Figure 4.12 Average three dimensional velocity distribution at the boundary region on investigation plane 5.....	58
Figure 5.1 Control volume of geometry.....	59
Figure 5.2 Mesh processing .....	60
Figure 5.3 Mesh processing .....	61
Figure 5.4 Momentum and mass residuals.....	62
Figure 5.5 Turbulence residuals.....	62
Figure 5.6 Distribution of average velocity values at the out flow section on investigation planes .....	64
Figure 5.7 Distribution of average velocity values at the out flow section on investigation planes .....	65
Figure 5.8 Design of baffles that are used for parametric study. ....	66
Figure 5.9 Model A parametric results. ....	67
Figure 5.10 Model B parametric results.....	68
Figure 5.11 Model C parametric results.....	69

## LIST OF TABLES

	<b>Page</b>
Table 2.1 Typical values of convection heat transfer coefficient .....	18
Table 4.1 Specifications of the PIV system components .....	48

## **CHAPTER ONE**

### **INTRODUCTION**

Domestic refrigerator is a common household appliance that is used short term preservation of foodstuff in the home. Basically a refrigerator consists of a thermally insulated compartment and a heat pump that transfers heat from the inside of the compartment to external ambient. Definition of refrigerator according to International Standard Organization (ISO 15502) is “factory-assembled insulated cabinet with one or more compartments and of suitable volume and equipment for household use, cooled by natural convection or a frost-free system whereby the cooling is obtained by one or more energy-consuming.” (ISO 15502:2005)

Domestic refrigerators are mainly categorized as Static, No\_Frost and Frost\_Free that is shown in Figure 1.1, according to occurrence of the inner air circulation. Static system is designed according to natural convection with different types of evaporators such as WOT (wire on tube) and POT (plate on tube) that are directly contact the inner air of compartment.

No\_Frost system commonly has a fin evaporator to absorb heat from all compartments and a fan to circulate the inner air between evaporator and compartment(s) by the effect of forced air convection.

Frost\_Free system is involved fans in order to absorb heat from the relevant compartment. There isn't any air transfer between the compartments. Forced air convection application for one compartment is enough to define a refrigerator as Frost\_Free.

In this study we focus on a radial fan, which is mounted on the back wall a Frost\_Free model refrigerator, was determined that there is an inappropriate flow characteristic at the exit region.

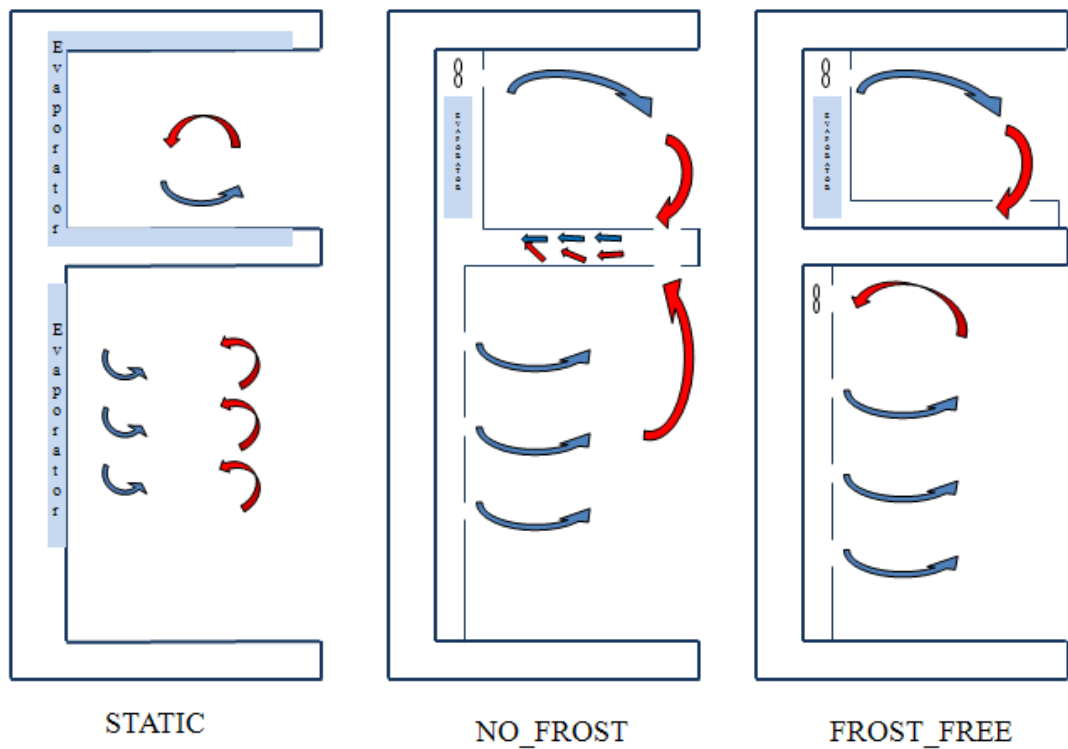


Figure 1.1 Cooling systems on domestic refrigerators.

The aim of this study is to optimizing the flow direction outlet the duct of the fan, which is mounted on the refrigerators' cooling compartment that is determined by experimental and numerical investigations, with using Particular Image Velocimetry (PIV) method and were analyzed to use the Computational Fluid Dynamics (CFD) method.

Flow characteristics' the fan model was determined that wasn't appropriate direction outlet the fan. Therefore duct design was decided to revise so as to correct the flow characteristic. Experimental study includes outlet data of full model to verify numerical study. Furthermore the duct of the model was cut off and experimental study was repeated. The cutoff models' outlet data was used as a boundary condition at revision study of the duct design. Revision study steps are given below;

- Measurement of full model outlet.
- Measurement of cutoff fan model outlet.
- Numerical study on the CAD design of duct with PIV data.

- Verification of CFD results according to PIV data.
- Optimization of flow characteristic with parametric study.

## 1.1 Literature Survey

Usage of the fan becomes widespread, according to rising client requirements and mandatory about the international standards on domestic refrigerator industry. Basically fans provide the temperature distribution in the refrigerator compartments or cycling the air between the compartments. Additionally, various types of fans are used to increase the thermal convection on the condenser or compressor in order to produce high efficiency refrigerators. According to all of these main reasons, fans and their locations are important inner design parameters on refrigerators. There is also some critical points on design parameters that restrict usage of fans such as acoustic and energy efficiency limits according to relevant standards.

In this paper, experimental and numerical studies were carried out on a radial fan that is used a refrigerator compartment with evaporator inside the backwall. First full PIV method was implemented on the radial fans' exit region as an experimental study. After the observation of the mean flow characteristic, second PIV measurement was carried out of cutoff model in order to use as a boundary condition in the numerical study of duct. Second step of study is to verify numerical study with experimental results Different types of baffle designs were applied in the duct according to obtained knowledge. Finally parametric study was carried out for three types of baffles to determine the convenient modification. As the parameters; angle and position of baffles were specify the flow distribution at the exit region. Main target of parametric study was to equalize the velocity distribution at the exit region of duct to increase the forced convection on the whole evaporator surface.

Seungyub Lee, Seung Heo, Cheolung Cheong (2010) mentioned the source of noise in refrigerators such as compressor and fan. Many studies using experimental and numerical methods have been carried out of fan noise and have contributed to a better understanding of the mechanisms of fan noise generation. In this study they

proposed a hybrid method consisting of three steps; CFD simulation, the Acoustic Analogy, and the boundary element method (BEM) for a centrifugal fan to modify the cutoff region that is the strongest source of aerodynamic noise because of unsteady flow in the fan case. Numerical approaches have been used to understand the unsteady flow fields and mechanisms. The unsteady flow field of the centrifugal fan in a duct is predicted by solving the incompressible Reynolds-averaged Navier-Stokes equations with conventional computational fluid dynamics techniques. Aero-acoustic sources were extracted from information on unsteady flow fields. Internal blade passing frequency (BPF) fan noise was predicted by combining the modeled sources with a tailored Green's function that considered the effects of duct walls on the propagation of sound waves. This was numerically realized using the BEM. A parametric study was performed to validate the effectiveness of the proposed method as a design tool. Finally sound pressure levels of the fundamental BPF of the modified centrifugal fans are predicted to be 2 to 3dB less than the original model.

It's well known that fans and compressors significantly contribute to the overall noise from a refrigerator. Fans in refrigerators are used for several purposes and also large sized refrigerators need higher volume flow rates. This high rotational speed increases the fan noise problem. Seung Heo, Cheolung Cheong, Tae-Hoon Kim (2011) focused on another main point that the inclined S-shaped fans reduce the noise against the existing fans. Noise reduction is support with hybrid CAA (computational aero acoustic) techniques which are carried out using the low-noise prototype fans. The hybrid method consists of three steps. First, the flow field is calculated through CFD. Second, the noise sources are modeled by using calculated flow field data through the acoustic analogy. Finally, acoustic field is predicted by combining the modeled noise sources with the wave equation, under the given internal duct boundary conditions. To assess the possible reduction in the broadband noise components, the turbulent kinetic energy of can be reduced by using inclined S-shaped trailing edge lines. Noise measurements are carried out using the low-noise prototype fans; the results show that the overall SPL values are reduced by 2-3.5dB when the rotational speed ranges from 1800 rpm to 2400 rpm. The results of the final experiment involving the full set of a refrigerator equipped with the final low noise

by approximately 2.2 dBA in the comparison with the existing fan. This study shows us the actual noise reduction mechanisms are affected by the coupled effects of the inclination and the S-shape, and are not independent of each other.

Shun-Chang Yen and Jung-Hsuan Liu (2007) used the PIV method to measure the instantaneous and ensemble average flow field on two different (diametral and lateral) planes in the near exit region. To design the centrifugal fans efficiently and optimally, the flow structures, velocity distributions, and flow rates were recorded and derived. The performance coefficients at different flow rates were calculated and compared by using the AMCA wind tunnel test. The different rotation speeds cause different phenomena in the exit region. These variations certainly influence the efficiency of the fans. The efficiency of Fan A that 3100rpm rotational speed is 3.95%. The efficiency of Fan B that 4000rpm rotational speed is 13.1%. The extra 9.15% comes from the speed effect under the conditions of identical geometrical structure and the same driving voltage. Additionally, the knowledge on this paper is discussing the relationship between the near-exit flow patterns and the efficiency parameters. These results can also be applied to the field of optimal design.

According to literature research numerical and experimental methods have been used the one within the other. Generally PIV method is preferred to validate numerical studies that are implemented for design parameters or used to determine the current situation. In this study as distinct from the ordinary implementations, PIV study was applied to both validate and obtain the boundary condition values for numerical study. Thus numerical study results would be more successful. This hybrid method makes the numerical design study more reliable as is presented in chapter five.



## **CHAPTER TWO**

### **REFRIGERATORS**

#### **1.1 History of Refrigerators Development**

The first known method of artificial refrigeration was demonstrated by William Cullen at the University of Glasgow in Scotland in 1756. Cullen used a pump to create a partial vacuum over a container of diethyl ether, which then boiled, absorbing heat from the surrounding air. The experiment even created a small amount of ice, but had no practical application at that time. (Refrigeration, n.d.)

In 1758, Benjamin Franklin and John Hadley, professor of chemistry at Cambridge University, conducted an experiment to explore the principle of evaporation as a means to rapidly cool an object. Franklin and Hadley confirmed evaporation of highly volatile liquids, such as alcohol and ether, could be used to drive down the temperature of an object past the freezing point of water. They conducted their experiment with the bulb of a mercury thermometer as their object and with a bellows used to “quicken” the evaporation; they lowered the temperature of the thermometer bulb down to 7°F (-14°C), while the ambient temperature was 65°F (18°C). Franklin noted that soon after they passed the freezing point of water (32°F), a thin film of ice formed on the surface of the thermometer’s bulb and that the ice mass was about a quarter inch thick when they stopped the experiment upon reaching 7°F (-14°C). Franklin concluded, “From this experiment, one may see the possibility of freezing a man to death on a warm summer’s day.”

In 1805, American inventor Oliver Evans designed, but never built, a refrigeration system based on the vapor-compression refrigeration cycle rather than chemical solutions or volatile liquids such as ethyl ether.

In 1820, the British scientist Michael Faraday liquefied ammonia and other gases by using high pressures and low temperatures.

An American living in Great Britain, Jacob Perkins obtained the first patent for vapor-compression refrigeration system in 1834. Perkins built a prototype system and it actually worked, although it did not succeed commercially.

In 1842, an American physician, John Gorrie, designed the first system to refrigerate water to produce ice. He also conceived the idea of using his refrigeration system to cool the air for comfort in homes and hospitals (i.e., air conditioning). His system compressed air, then partly cooled the hot compressed air with water before allowing it to expand while doing part of the work needed to drive the air compressor. That isentropic expansion cooled the air to a temperature low enough to freeze water and produce ice or to flow “through a pipe for effecting refrigeration otherwise” as stated in his patent granted by the U.S. Patent Office in 1851. Gorrie built a working prototype, but his system was a commercial failure.

Alexander Twining began experimenting with vapor-compression refrigeration in 1848, and obtained patents in 1850 and 1853. He is credited with having initiated commercial refrigeration in the United States by 1856.

Meanwhile in Australia, James Harrison began operation of a mechanical ice-making machine in 1851 on the banks of the Barwon River at Rocky Point in Geelong, Victoria. His first commercial ice-making machine followed in 1854, and his patent for an ether liquid-vapour compression refrigeration system was granted in 1855. Harrison introduced commercial vapour-compression refrigeration to breweries and meat packing houses, and by 1861, a dozen of his systems were in operation.

Australian, Argentine and American concerns experimented with refrigerated shipping in the mid 1870s; the first commercial success came when William Soltau Davidson fitted a compression refrigeration unit to the New Zealand vessel Dunedin in 1882, leading to a meat and dairy boom in Australasia and South America. J&E Hall of Dartford, England outfitted the ‘SS Selebria’ with a vapor compression system to bring 30,000 carcasses of mutton from the Falkland Islands in 1886.

The first gas absorption refrigeration system using gaseous ammonia dissolved in water (referred to as “aqua ammonia”) was developed by Ferdinand Carre of France in 1859 and patented in 1860. The Servel company built gas powered, absorption refrigerators in Evansville, IN from 1927 through built gas powered, absorption refrigerators in Evansville, IN from 1927 through 1956. In the United States, the consumer public at that time still used the ice box with ice brought in from commercial suppliers, many of whom were still harvesting ice and storing it in an icehouse.

Thaddeus Lowe, an American balloonist from the Civil War, had experimented over the years with the properties of gases. One of his mainstay enterprises was the high-volume production of hydrogen gas. He also held several patents on ice-making machines. His “Compression Ice Machine” would revolutionize the cold storage industry. In 1869, other investors and he purchased an old steamship onto which they loaded one of Lowe’s refrigeration units, and began shipping fresh fruit from New York to the Gulf Coast area, and fresh meat from Galveston, Texas back to New York. Because of Lowe’s lack of knowledge about shipping, the business was a costly failure, and it was difficult for the public to get used to the idea of being able to consume meat that had been so long out of the packing house.

Domestic mechanical refrigerators became available in the United States around 1911.

## **1.2 Domestic Refrigerating System Basics and Theories**

Refrigeration is one of the most important thermal processes in various practical applications, ranging from space conditioning to food cooling. In these systems, the refrigerant is used to transfer the heat. Initially, the refrigerant absorbs heat because its temperature is lower than the heat source’s temperature and the temperature of the refrigerant is increased during the process to a temperature higher than the heat sink’s temperature. Therefore, the refrigerant delivers the heat.

In domestic refrigerators, vapor-compression systems are the most commonly used refrigeration systems and each systems employs a compressor (Dincer & Kanoglu, 2010).

### ***1.2.1 The Ideal Vapor-Compression Refrigeration Cycle***

The main goal of a refrigeration system which performs the reverse effect of a heat engine is to remove the heat from a low-level temperature medium as a heat source and to transfer this heat to a higher level temperature medium as a heat sink. Figure 2.1 shows a thermodynamic system acting as refrigeration machine. The absolute temperature of the source is  $T_L$  and the heat transferred from the source is the refrigeration effect (refrigeration load)  $Q_L$ . On the other side, the heat rejection to the sink at the temperature  $T_H$  is  $Q_H$ . Both effects are accomplished by the work input  $W$ . For continuous operation, the first law of thermodynamics is applied to the system

Many of the impracticalities associated with the reversed Carnot cycle can be eliminated by vaporizing the refrigerant completely before it is compressed and by replacing the turbine with a throttling device, such as an expansion valve or capillary tube. The cycle that results is called the ideal vapor-compression refrigeration cycle, and it is shown schematically and on a  $T-s$  diagram in Figure 2.1. The vapor compression refrigeration cycle is the most widely used cycle for refrigerators, air conditioning systems, and heat pumps. It consists of four processes (Cengel & Boles, 2006):

- 1-2 Isentropic compression in a compressor
- 2-3 Constant-pressure heat rejection in a condenser
- 3-4 Throttling in an expansion device
- 4-1 Constant-pressure heat absorption in an evaporator

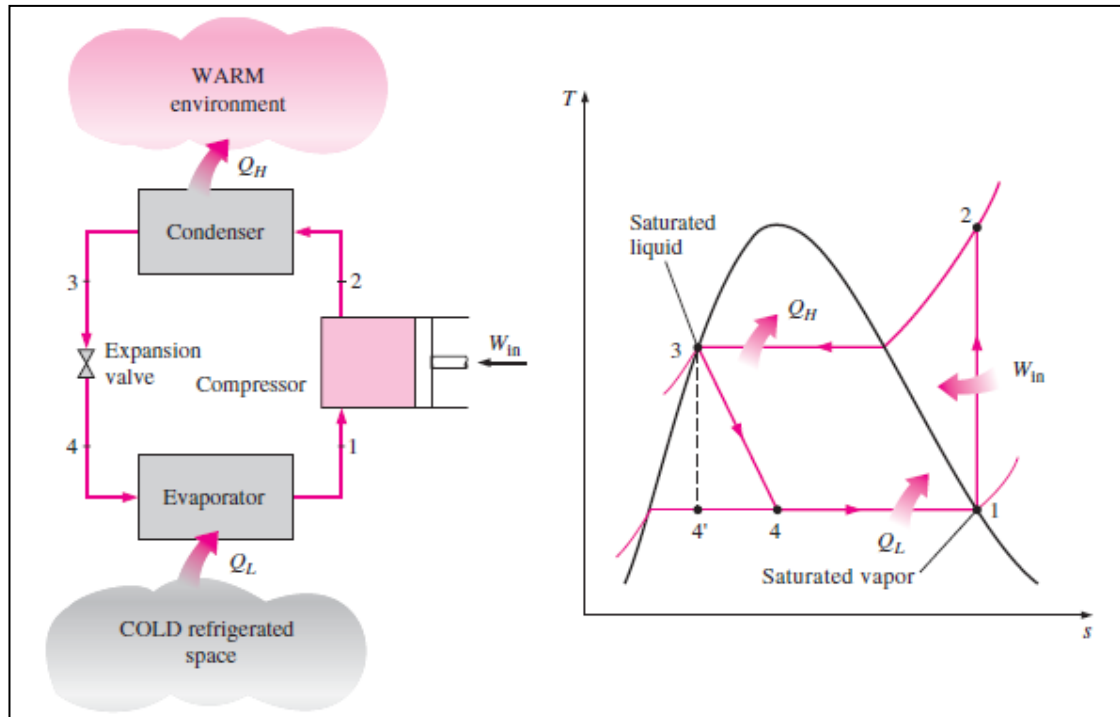


Figure 2.1 Schematic T-s diagram for the ideal vapor-compression refrigeration cycle (Cengel & Boles, 2006).

In an ideal vapor-compression refrigeration cycle, the refrigerant enters the compressor at state 1 as saturated vapor and is compressed isentropically to the condenser pressure. The temperature of the refrigerant increases during this isentropic compression process to well above the temperature of the surrounding medium. The refrigerant then enters the condenser as vapor at state 2 and leaves as saturated liquid at state 3 as a result of heat rejection to the surroundings. The temperature of the refrigerant at this state is still above the temperature of the surroundings.

The saturated liquid refrigerant at state 3 is throttled to the evaporator pressure by passing it through an expansion valve or capillary tube. The temperature of the refrigerant drops below the temperature of the refrigerated space during this process. The refrigerant enters the evaporator at state 4 as a low-quality saturated mixture, and it completely evaporates by absorbing heat from the refrigerated space. The refrigerant leaves the evaporator as saturated vapor and reenters the compressor, completing the cycle.

In a household refrigerator (Figure 2.2), the tubes in the freezer compartment where heat is absorbed by the refrigerant serves as the evaporator. The coils behind the refrigerator, where heat is dissipated to the kitchen air, serve as the condenser.

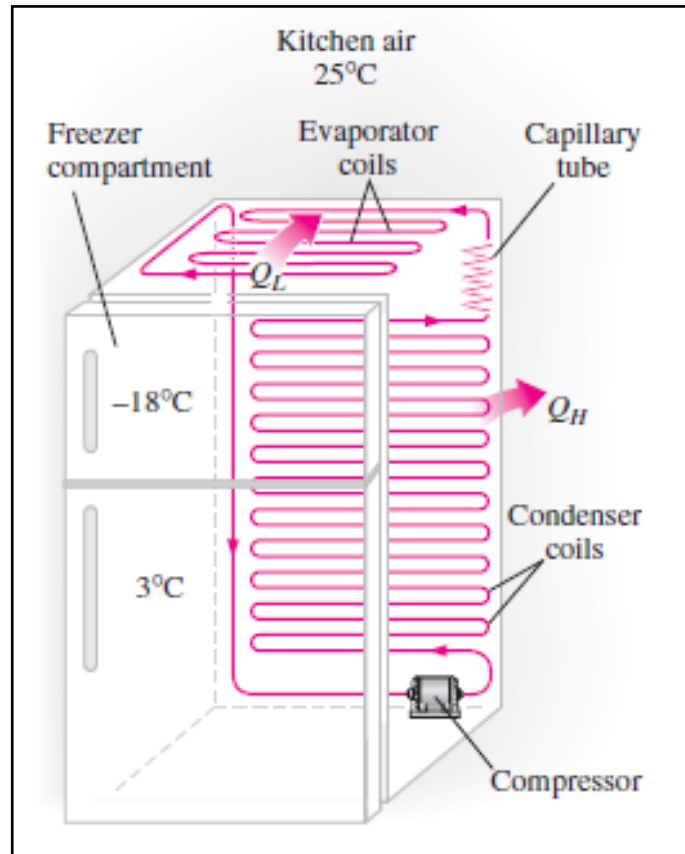


Figure 2.2 An ordinary household refrigerator (Cengel & Boles, 2006).

The area under the process curve 4-1 represents the heat absorbed by the refrigerant in the evaporator, and the area under the process curve 2-3 represents the heat rejected in the condenser. A rule of thumb is that the COP improves by 2 to 4 percent for each  $^{\circ}\text{C}$  the evaporating temperature is raised or the condensing temperature is lowered.

Another diagram frequently used in the analysis of vapor-compression refrigeration cycles is the  $P-h$  diagram, as shown in Figure 2.3. On this diagram, three of the four processes appear as straight lines, and the heat transfer in the condenser and the evaporator is proportional to the lengths of the corresponding process curves.

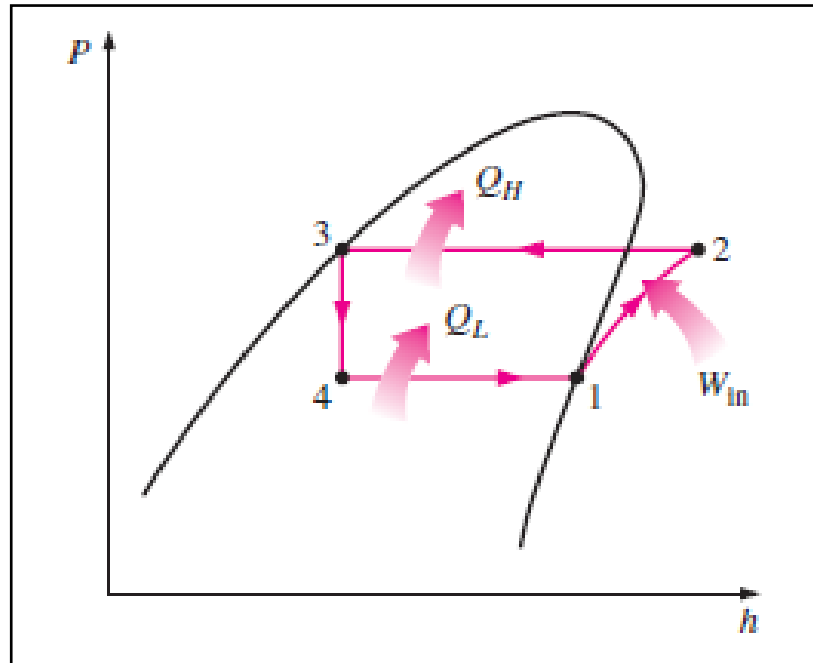


Figure 2.3 The P-h diagram of an ideal vapor-compression refrigeration cycle (Cengel & Boles, 2006).

The ideal vapor compression refrigeration cycle is not an internally reversible cycle since it involves an irreversible (throttling) process. This process is maintained in the cycle to make it a more realistic model for the actual vapor-compression refrigeration cycle. If the throttling device were replaced by an isentropic turbine, the refrigerant would enter the evaporator at state 4' instead of state 4. As a result, the refrigeration capacity would increase (by the area under process curve 4'-4 in Figure 2.1) and the network input would decrease (by the amount of work output of the turbine). Replacing the expansion valve by a turbine is not practical, however, since the added benefits cannot justify the added cost and complexity.

All four components associated with the vapor-compression refrigeration cycle are steady-flow devices, and thus all four processes that make up the cycle can be analyzed as steady-flow processes. The kinetic and potential energy changes of the refrigerant are usually small relative to the work and heat transfer terms, and therefore they can be neglected. Then the steady flow energy equation on a unit-mass basis reduces to

$$(q_{in} - q_{out}) + (w_{in} - w_{out}) = h_e \quad (2.1)$$

The condenser and the evaporator do not involve any work, and the compressor can be approximated as adiabatic. Then the COPs of refrigerators and heat pumps operating on the vapor-compression refrigeration cycle can be expressed as

$$COP_R = \frac{q_L}{w_{net,in}} = \frac{h_1 - h_4}{h_2 - h_1} \quad (2.2)$$

$$COP_{HP} = \frac{q_H}{w_{net,in}} = \frac{h_2 - h_3}{h_2 - h_1} \quad (2.3)$$

where  $h_1 = h_{g@P_1}$  and  $h_3 = h_{g@P_3}$  for ideal case.

### ***1.2.2 Actual Vapor-Compression Refrigeration Cycle***

An actual vapor-compression refrigeration cycle differs from the ideal one in several ways, owing mostly to the irreversibilities that occur in various components. Two common sources of irreversibilities are fluid friction (causes pressure drops) and heat transfer to or from the surroundings. The  $T$ - $s$  diagram of an actual vapor-compression refrigeration cycle is shown in Figure 2.4.

In the ideal cycle, the refrigerant leaves the evaporator and enters the compressor as saturated vapor. In practice, however, it may not be possible to control the state of the refrigerant so precisely. Instead, it is easier to design the system so that the refrigerant is slightly superheated at the compressor inlet. This slight overdesign ensures that the refrigerant is completely vaporized when it enters the compressor. Also, the line connecting the evaporator to the compressor is usually very long; thus the pressure drop caused by fluid friction and heat transfer from the surroundings to the refrigerant can be very significant.



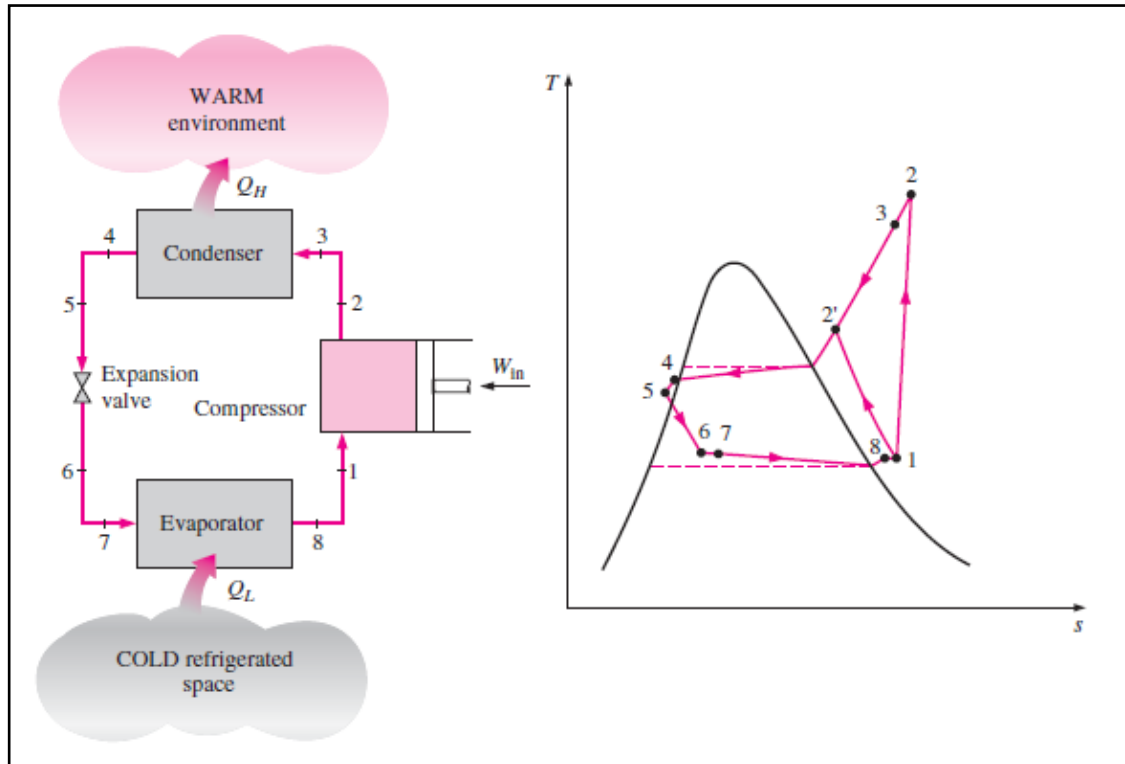


Figure 2.4 Schematic and T-s diagram for the actual vapor-compression refrigeration cycle (Cengel & Boles, 2006).

The result of superheating, heat gain in the connecting line, and pressure drops in the evaporator and the connecting line is an increase in the specific volume, thus an increase in the power input requirements to the compressor since steady-flow work is proportional to the specific volume.

The compression process in the ideal cycle is internally reversible and adiabatic, and thus isentropic. The actual compression process, however, involves frictional effects, which increase the entropy, and heat transfer, which may increase or decrease the entropy, depending on the direction. Therefore, the entropy of the refrigerant may increase (process 1-2) or decrease (process 1-2') during an actual compression process, depending on which effects dominate. The compression process 1-2' may be even more desirable than the isentropic compression process since the specific volume of the refrigerant and thus the work input requirement are smaller in this case. Therefore, the refrigerant should be cooled during the compression process whenever it is practical and economical to do so.

In the ideal case, the refrigerant is assumed to leave the condenser as saturated liquid at the compressor exit pressure. In reality, however, it is unavoidable to have some pressure drop in the condenser as well as in the lines connecting the condenser to the compressor and to the throttling valve. Also, it is not easy to execute the condensation process with such precision that the refrigerant is a saturated liquid at the end, and it is undesirable to route the refrigerant to the throttling valve before the refrigerant is completely condensed. Therefore, the refrigerant is sub-cooled somewhat before it enters the throttling valve. We do not mind this at all, however, since the refrigerant in this case enters the evaporator with a lower enthalpy and thus can absorb more heat from the refrigerated space. The throttling valve and the evaporator are usually located very close to each other, so the pressure drop in the connecting line is small.

### **1.3 Heat Transfer Mechanisms**

As we defined the heat transfer on refrigerator systems previously topics, energy can be transferred from one system to another as a result of temperature difference. A thermodynamic analysis is concerned with the amount of heat transfer as a system undergoes a process from one equilibrium state to another. The determination of the rates of such energy transfers is the heat transfer. The transfer of the energy as heat is always from the higher temperature medium to the lower temperature one, and heat transfer stops when the two mediums reach the same temperature.

Heat can be transferred in three different modes: conduction, convection and radiation. All modes of heat transfer require the existence of a temperature difference, and all modes are from the high temperature medium to a lower temperature one.

Conduction is the transfer of energy from the more energetic particles of a substance to the adjacent less energetic ones as a result of interactions between the particles. Conduction can take place in solids, liquids or gases. In gases and liquids,

conduction is due to the collisions and diffusion of the molecules during their random motion.

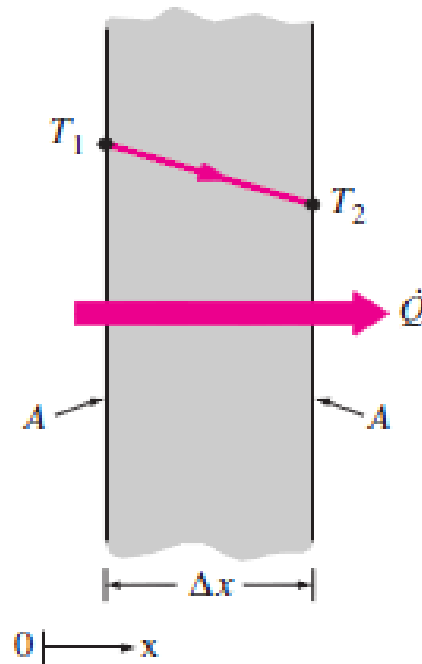


Figure 2.5 Heat conduction through a large plane wall of thickness  $\Delta x$  and area  $A$  (Cengel & Boles, 2006).

Consider steady heat conduction through a large plane wall of thickness  $\Delta x=L$  and area  $A$ , as shown in Figure 2.5. The temperature difference across the wall is  $\Delta T = T_2 - T_1$ . Experiments have shown that the rate of heat transfer  $Q$  through the wall is doubled when the temperature difference  $\Delta T$  across the wall or the area  $A$  normal to the direction of heat transfer is doubled, but is halved when the wall thickness  $L$  is doubled. Thus we conclude that the rate of heat conduction through a plane layer is proportional to the temperature difference across the layer and the heat transfer area, but is inversely proportional to the thickness of the layer. That is,

$$\text{Rate of heat conduction} \propto \frac{(\text{Area})(\text{Temperature difference})}{\text{Thickness}}$$

$$\dot{Q}_{\text{cond}} = kA \frac{T_1 - T_2}{\Delta x} = -kA \frac{\Delta T}{\Delta x} \quad (\text{W}) \quad (2.4)$$

where the constant of proportionality  $k$  is the thermal conductivity of the material, which is measure of the ability of a material to conduct heat.

Convection is the mode of energy transfer between a solid surface and the adjacent liquid or gas that is in motion, and it involves the combine effects of conduction and fluid motion. The faster the fluid motion, the greater the convection heat transfer. In the absence of any bulk fluid motion, heat transfer between a solid surface and the adjacent fluid enhances the heat transfer between the solid surface and the fluid, but it also complicates the determination of heat transfer rates.

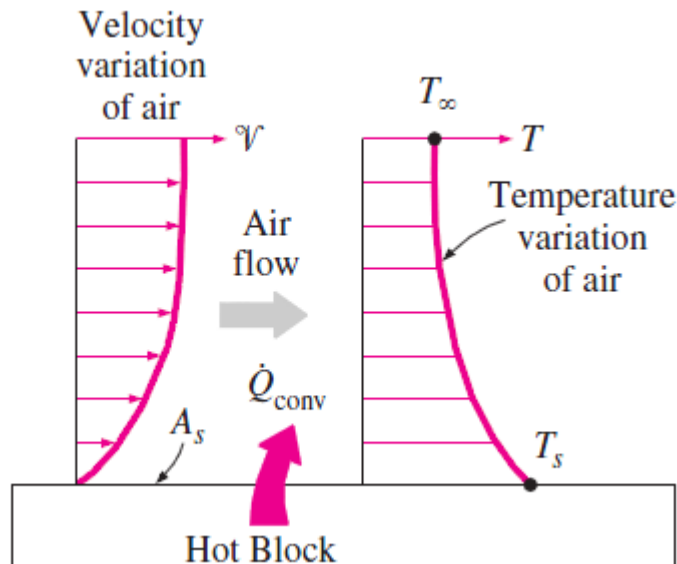


Figure 2.6 Heat transfer from a hot surface to air by convection (Cengel & Boles, 2006).

Consider the cooling of hot block by blowing cool air over its top surface (Figure 2.6). Energy is first transferred to the air layer adjacent to the block by conduction. This energy is then carried away from the surface by convection, that is, by the combined effects of conduction within the air that is due to random motion of air molecules and the bulk or macroscopic motion of the air that removes the heated air near the surface and replaces it by the cooler air.

Convection is called forced convection if the fluid is forced to flow over the surface by external means such as a fan, pump, or the wind. In contrast, convection is

called natural convection if the fluid motion is caused by buoyancy forces that are induced by density differences due to the variation of temperature in fluid.

Despite the complexity of convection, the rate of convection heat transfer is observed to be proportional to the temperature difference, and is conveniently expressed by Newton's law of cooling as where  $h$  is the convection heat transfer coefficient in  $W/m^2 \cdot ^\circ C$ .

$$Q_{conv} = hA_s(T_s - T_\infty) \quad (W) \quad (2.5)$$

$A_s$  is the surface area through which convection heat transfer takes place,  $T_s$  is the surface temperature, and  $T_\infty$  is the temperature of the fluid sufficiently far from the surface.

The convection heat transfer coefficient  $h$  is not a property of the fluid. It is an experimentally determined parameter whose value depends on all the variables influencing convection such as surface geometry, the nature of fluid motion, the properties of the fluid, and the bulk fluid velocity. Typical values of  $h$  are given in Table 2.1.

Table 2.1 Typical values of convection heat transfer coefficient (Cengel & Boles, 2006).

Type of convection	$h, W/m^2 \cdot ^\circ C$
Free convection of gases	2-25
Free convection of liquids	10-1000
Forced convection of gases	25-250
Forced convection of liquids	50-20.000
Boiling and condensation	2500-100.000

Radiation is the energy emitted by matter in the form of electromagnetic waves as a result of the changes in the electronic configurations of the atoms or molecules. Unlike conduction and convection, the transfer of energy by radiation does not require the presence of an intervening medium. In fact, energy transfer by radiation is fastest and it suffers no attenuation in a vacuum. This how the energy of the sun reaches the earth.

In heat transfer studies we are interested in thermal radiation, which is the form of radiation emitted by bodies because of their temperature. It differs from other forms of electromagnetic radiation such as x-rays, gamma rays, microwaves, radio waves and television waves that are not related to temperature. All bodies at a temperature above absolute zero emit thermal radiation.

Radiation is a volumetric phenomenon, and all solids, liquids and gases emit, absorb or transmit radiation to varying degrees. However, radiation is usually considered to be a surface phenomenon for solids that are opaque to thermal radiation such as metals, wood and rocks since the radiation emitted by the interior regions of such material can never reach the surface and the radiation incident on such bodies is usually absorbed within a few microns from the surface.

The maximum rate of radiation that can be emitted from a surface at an absolute temperature  $T_s$  is given by Stefan-Boltzmann law as where  $\sigma=5.67 \times 10^{-8} \text{ W/m}^2 \cdot \text{K}$  is the Stefan-Boltzmann constant.

$$Q_{\text{emit,max}} = \sigma A_s T_s^4 \quad (\text{W}) \quad (2.6)$$

The idealized surface that emits radiation at this maximum rate is called a blackbody and the radiation emitted by blackbody is called blackbody radiation (Figure 2.7)

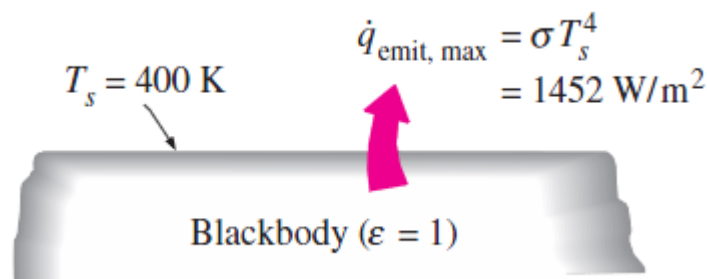


Figure 2.7 Blackbody radiation represents the maximum amount of radiation that can be emitted from a surface at a specified temperature. (Cengel & Boles, 2006).

The radiation emitted by all real surfaces is less than the radiation emitted by blackbody at the temperature, and is expressed as where  $\epsilon$  is the emissivity of the surface.

$$\dot{Q}_{\text{emit}} = \epsilon \sigma A_s T_s^4 \quad (\text{W}) \quad (2.7)$$

The property emissivity, whose value is in the range  $0 \leq \epsilon \leq 1$ , is a measure of how closely a surface approximates a blackbody for which  $\epsilon = 1$ .

### ***1.3.1 Physical Mechanism of Convection***

Experience shows that convection heat transfer strongly depends on the fluid properties dynamic viscosity  $\mu$ , thermal conductivity  $k$ , density  $\rho$  and specific heat  $C_p$  as well as the fluid velocity  $V$ . It also depends on the geometry and the roughness of the solid surface, in addition to the type of fluid flow such as being streamlined or turbulent. Thus, we expect the convection heat transfer relations to be rather complex because of the dependence of convection on so many variables. This is not surprising, since convection is the most complex mechanism of heat transfer.

Despite the complexity of convection, the rate of convection heat transfer is observed to be proportional to the temperature difference and is conveniently expressed by Newton's law of cooling as

$$q_{\text{conv}} = h(T_s - T_\infty) \quad (\text{W/m}^2) \quad (2.8)$$

When a fluid is forced to flow over a solid surface that is nonporous, it is observed that the fluid in motion comes to a complete stop at the surface and assumes a zero velocity relative to the surface. That is, the fluid layer in direct contact with a solid surface to the surface and there is no slip. In fluid flow, this phenomenon is known as the no-slip condition, and it is due to the viscosity of the fluid (Figure 2.8).

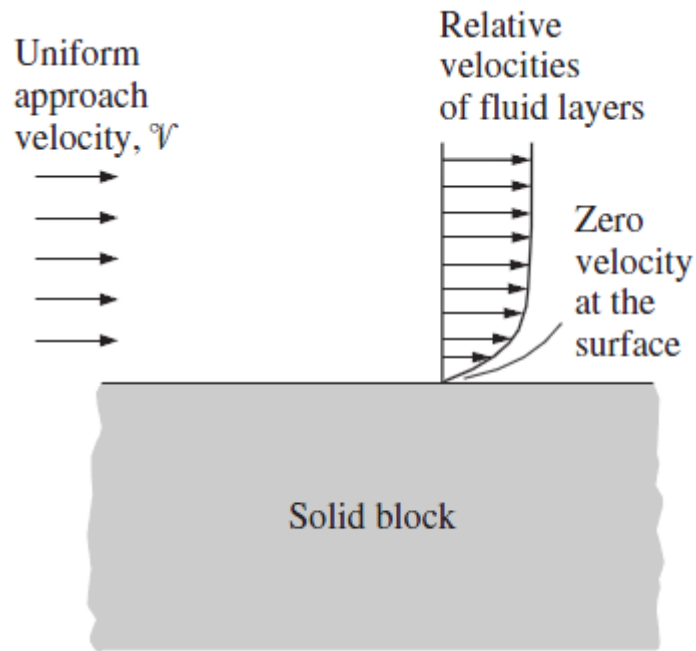


Figure 2.8 A fluid flowing over a stationary surface comes to a complete stop at the surface because of the no-slip condition. (Cengel & Boles, 2006).

Because of the friction between the fluid layers, velocity profiles must have zero values at the points of the points of contact between a fluid and a solid. When two bodies at different temperatures are brought into contact, heat transfer occurs until both bodies assume the same temperature at the point of contact. This is known as no-temperature-jump condition.

An implication of the no-slip and the no-temperature jump conditions is that heat transfer from the solid surface to the fluid layer adjacent to the surface is by pure conduction, since the fluid layer is motionless, and can be expressed as where  $T$  represents the temperature distribution in the fluid and  $(dT/dY)_{y=0}$  is the temperature gradient at the surface.

$$\dot{q}_{\text{conv}} = \dot{q}_{\text{cond}} = -k_{\text{fluid}} \left. \frac{\delta T}{\delta y} \right|_{y=0} \quad (\text{W/m}^2) \quad (2.9)$$

Convection heat transfer from a solid surface to the fluid is merely the conduction heat transfer from the solid surface to the fluid layer adjacent to the surface.



Therefore we can equate the equations 1.8 and 1.9 for the heat flux to obtain for the determination of the convection heat transfer coefficient when the temperature distribution within the fluid is known.

$$h = \frac{-k_{\text{fluid}} (\delta T / \delta y)_{y=0}}{T_s - T_\infty} \quad \left( \frac{\text{W}}{\text{m}^2 \cdot ^\circ\text{C}} \right) \quad (2.10)$$

### 1.3.1.1 Nusselt Number

Wilhelm Nusselt, who made significant contributions to convective heat transfer in the first half of the twentieth century and it is viewed as the dimensionless convection heat transfer coefficient.

$$Nu = \frac{hL_c}{k} \quad (2.11)$$

Heat transfer through the fluid layer will be by convection when the fluid involves some motion and by conduction when the fluid layer is motionless. The ratio of heat flux that is the rate of heat transfer per unit time per unit surface area, either convection to conduction gives Nusselt number.

$$\frac{\dot{q}_{\text{conv}}}{\dot{q}_{\text{cond}}} = \frac{h\Delta T}{k\Delta T/L} = \frac{hL}{k} = Nu \quad (2.12)$$

### 1.3.1.2 Prandtl Number

Consider the parallel flow of a fluid over a flat plate, as shown in Figure 2.9. The region of the flow above the plate bounded by  $\delta$  in which the effects of the viscous shearing forces caused by fluid viscosity are felt is called the velocity boundary layer. The boundary layer thickness is typically defined as the distance  $y$  from the surface at which  $u=0.99u_\infty$ . Also we can explain the thermal boundary layer same definition such as uniform temperature instead of parallel flow. Thus, the flow region over the surface in which the temperature variation in the direction normal to the surface is significant is the thermal boundary layer.

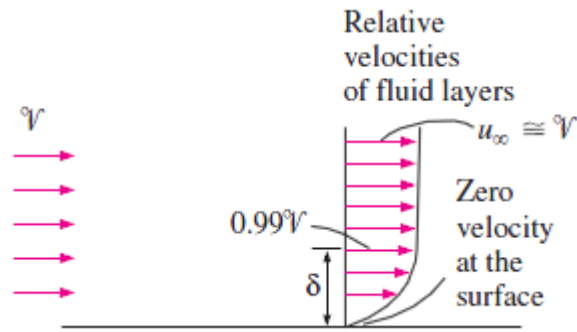


Figure 2.9 The development of a boundary layer on a surface is due to the no-slip condition. (Cengel & Boles, 2006).

The relative thickness of the velocity and the thermal boundary layers is described by the dimensionless parameter Prandtl number, defined at equation below.

$$\text{Pr} = \frac{\text{Molecular diffusivity of momentum}}{\text{Molecular diffusivity of heat}} = \frac{\vartheta}{\alpha} = \frac{\mu c_p}{k} \quad (2.13)$$

The Prandtl numbers of fluids range from less than 0.01 for liquid metals to more than 100.000 for heavy oils and 10 for water. The Prandtl number of gases is about 1, which indicates that both momentum and heat dissipate through the fluid at about the same rate. Consequently the thermal boundary layer is much thicker for liquid metals and much thinner for oils relative to the velocity boundary layer.

### 1.3.1.3 Reynolds Number

The Reynolds number is defined as the ratio of inertial forces to viscous forces and consequently quantifies the relative importance of these two types of forces for given flow conditions. It's also a dimensionless quantity shown in equation 2.14.

$$\text{Re} = \frac{\text{Inertial forces}}{\text{Viscous forces}} = \frac{VL_c}{\vartheta} = \frac{\rho VL_c}{\mu} \quad (2.14)$$

V is the upstream velocity;  $L_c$  is the characteristic length of the geometry and  $\vartheta = \mu/\rho$  is the kinematic viscosity of the fluid. The Reynolds number at which the flow becomes turbulent is called the critical Reynolds number. The value of the

critical Reynolds number is different for all geometries. Generally for a flat plate, it's accepted  $5 \times 10^5$ , at which transition from laminar to turbulent flow occurs.

#### *1.3.1.4 Grashof Number*

The Grashof number is a dimensionless number in fluid dynamics and heat transfer which approximates the ratio of the buoyancy to viscous force acting on a fluid. It frequently arises in the study of situations involving natural convection.

$$Gr_L = \frac{g\beta(T_s - T_\infty)L_c^3}{\nu^2} \quad (2.15)$$

The role play by the Reynolds number in forced convection is played by the Grashof number in natural convection. As such, the Grashof number provides the main criteria in determining whether the fluid flow is laminar or turbulent in natural convection. For vertical plates, for example, the critical Grashof number is observed to be about  $10^9$ . Therefore, the flow regime on a vertical plate becomes turbulent at Grashof numbers greater than  $10^9$ .

When a surface is subjected to external flow, the problem involves both natural and forced convection. The relative importance of each mode of heat transfer is determined by the value of the coefficient  $Gr_L/Re_L^2$ . Natural convection effects are negligible if  $Gr_L/Re_L^2 \ll 1$ , free convection dominates and the forced convection effects are negligible if  $Gr_L/Re_L^2 \gg 1$ , and both effects are significant and must be considered if  $Gr_L/Re_L^2 \approx 1$ .

#### *1.3.1.5 Rayleigh Number*

The complexities of fluid motion make it very difficult to obtain simple analytical relations for heat transfer by solving the governing equations of motion and energy. Exceptions of some simple cases, heat transfer relations in natural convection are based on experimental studies. The simple empirical correlations for the average Nusselt number in natural convection, are of the form is given equation 2.16.

$$Nu = \frac{hL_c}{k} = C(Gr_L Pr)^n = CRa_L^n \quad (2.16)$$

The Rayleigh number which is the product of the Grashof and Prandtl number, for a fluid is a dimensionless number associated with buoyancy driven flow. The values of the constants C and n depend on the geometry of the surface and the flow regime, which is characterized by the range of the Rayleigh number. The value of “n” is usually 1/4 for laminar flow and 1/3 for turbulent flow. The value of the constant C is normally less than 1 (Cengel & Boles, 2002).

## 2.4 Domestic Refrigerators

The vapor-compression refrigerating systems used with modern refrigerators vary considerably in capacity and complexity, depending on the refrigerating application. They are hermetically sealed and normally require no replenishment of refrigerant or oil during the appliance’s useful life. The components of the system must provide optimum overall performance and reliability at minimum cost. In addition, all safety requirements of the appropriate safety standard (e.g., IEC Standard 60335-2-24, UL Standard 250) must be met. The fully halogenated refrigerant R-12 was used in household refrigerators for many years. However, because of its strong ozone depletion property, appliance manufacturers have replaced R-12 with environmentally acceptable R-134a or isobutene (ASHRAE, 2006).

In household refrigerators, vapor-compression refrigeration circuit (Figure 2.10) has five major components and some auxiliary equipment associated with these major components. These are compressor, condenser, evaporator, capillary tube (expansion valve) and refrigerant.

Figure 2.10 shows a common refrigerant circuit for a vapor compression refrigerating system. In the refrigeration cycle,

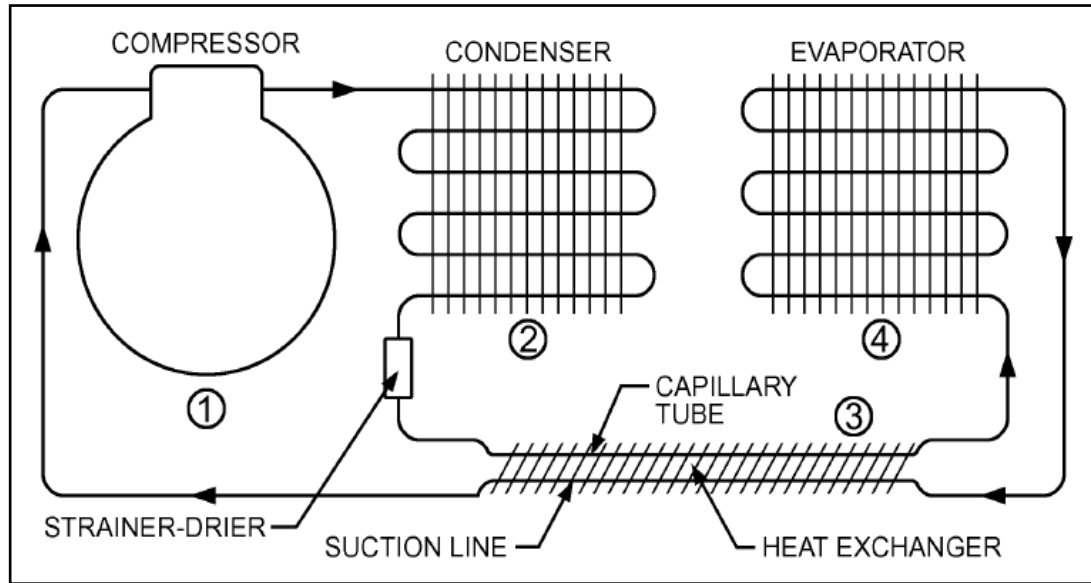


Figure 2.10 Refrigeration circuit (ASHRAE, 2006).

1. Electrical energy supplied to the motor drives a positive displacement compressor, which draws cold, low-pressure refrigerant vapor from the evaporator and compresses it.

2. The resulting high-pressure, high-temperature discharge gas then passes through the condenser, where it is condensed to a liquid while heat is rejected to the ambient air.

3. Liquid refrigerant passes through a metering (pressure-reducing) capillary tube to the evaporator, which is at low pressure.

4. The low-pressure, low-temperature liquid in the evaporator absorbs heat from its surroundings, evaporating to a gas, which is again withdrawn by the compressor.

### 2.4.1 Compressor

In a refrigeration cycle, the compressor has two main functions within the refrigeration cycle. One function is to pump the refrigerant vapor from the evaporator so that the desired temperature and pressure can be maintained in the evaporator. The second function is to increase the pressure of the refrigerant vapor through the process of compression, and simultaneously increase the temperature of the refrigerant vapor. By this change in pressure the superheated refrigerant flows through the system (Dincer & Kanoglu, 2010).

Refrigerant compressors, which are known as the heart of the vapor-compression refrigeration systems, can be divided into two main categories: displacement compressors and dynamic compressors. Both displacement and dynamic compressors can be hermetic, semi hermetic or open types.

The compressor both pumps refrigerant round the circuit and produces the required substantial increase in the pressure of the refrigerant. The refrigerant chosen and the operating temperature range needed for heat pumping generally lead to a need for a compressor to provide a high pressure difference for moderate flow rates, and this is most often met by a positive displacement compressor using a reciprocating piston. Other types of positive displacement compressor use rotating vanes or cylinders or intermeshing screws to move the refrigerant. In some larger applications, centrifugal or turbine compressors are used, which are not positive displacement machines but accelerate the refrigerant vapor as it passes through the compressor housing.

In the application, there are many different types of compressors available, in terms of both enclosure type and compression system. Here are some options for evaluating the most common types:

Reciprocating compressors are positive displacement machines, available for every application. The efficiency of the valve systems has been improved significantly on many larger models. Capacity control is usually by cylinder unloading (a method which reduces the power consumption almost in line with the capacity).

Scroll compressors are rotary positive displacement machines with a constant volume ratio. They have good efficiencies for air conditioning and high-temperature refrigeration applications. They are only available for commercial applications and do not usually have inbuilt capacity control.

Screw compressors are available in large commercial and industrial sizes and are generally fixed volume ratio machines. Selection of a compressor with the incorrect volume ratio can result in a significant reduction in efficiency. Part-load operation is achieved by a slide valve or lift valve unloading. Both types give a greater reduction in efficiency on part load than the reciprocating capacity control systems.

The refrigerant compressors are expected to meet these requirements: high reliability, long service life, easy maintenance, easy capacity control, quiet operation, compactness and cost effectiveness.

In the selection of a proper refrigerant compressor, these criteria are considered: refrigeration capacity, volumetric flow rate, and compression rate, thermal and physical properties of refrigerant. Thus, hermetic compressors are convenient for refrigerators. These compressors are preferable on reliability grounds to units primarily designed for the smaller range of temperatures required in household applications. In small equipment where cost is a major factor and on-site installation is preferably kept to a minimum, such as hermetically sealed motor/compressor combinations (Figure 2.11), there are no rotating seals separating motor and compressor, and the internal components are not accessible for maintenance, the casing being factory welded.

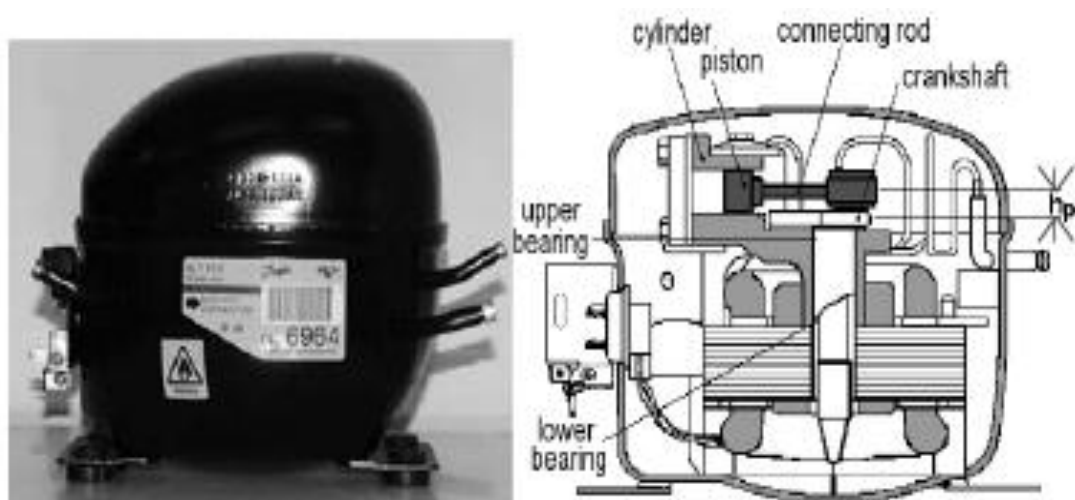


Figure 2.11 A typical hermetic compressor (Compressor, n.d.).

In these compressors, which are available for small capacities, motor and drive are sealed in compact welded housing. The refrigerant and lubricating oil are contained in this housing. Almost all small motor-compressor pairs used in domestic refrigerators and freezers are of the hermetic type. An internal view of a hermetic type refrigeration compressor is shown in Figure 1.7. The capacities of these compressors are identified with their motor capacities. For example, the compressor capacity ranges from 1/12 HP to 30BG in household refrigerators. Their revolutions per minute are either 1450 or 2800 rpm.



Figure 2.12 New, high-efficient compact coil air-cooled condensing units using hermetic compressors (Reciprocating Compressor, n.d.).

Hermetic compressors can work for a long time in small-capacity refrigeration systems without any maintenance requirement and without any gas leakage, but they are sensitive to electric voltage fluctuations, which may make the copper coils of the motor burn. The cost of these compressors is very low. Also, Figure 2.12 shows two air-cooled condensing units using a hermetic type refrigeration compressor.

### ***2.4.2 Condenser***

The condenser is the main heat rejecting component in the refrigerating system. It may be cooled by natural draft on free-standing refrigerators and freezers or fan cooled on larger models and on models designed for built-in applications (ASHRAE Refrigeration, 2006).



The natural-draft (Figure 2.13) condenser is located on the back wall of the cabinet and is cooled by natural air convection under the cabinet and up the back. The most common form consists of a flat serpentine of steel tubing with steel cross wires welded on 6 mm centers on one or both sides' perpendicular to the tubing. Tube-on sheet construction may also be used

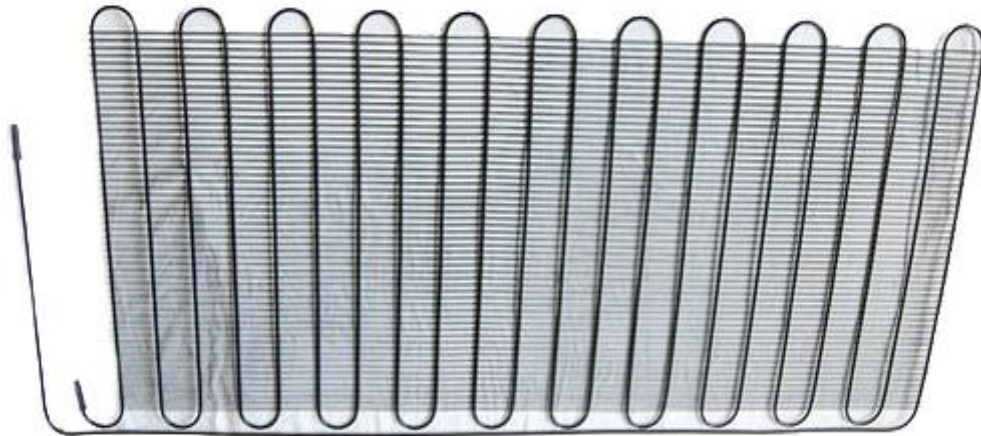


Figure 2.13 Schematic of a natural draft condenser (Static Condenser, n.d.).

The hot-wall condenser, another common natural-draft arrangement, consists of condenser tubing attached to the inside surface of the cabinet shell. The shell thus acts as an extended surface for heat dissipation. With this construction, external sweating is seldom a problem.

The forced-draft condenser (Figure 2.14) may be of fin-and-tube, folded banks of tube-and-wire, or tube-and-sheet construction. Various forms of condenser construction are used to minimize clogging caused by household dust and lint. The compact, fan-cooled condensers are usually designed for low airflow rates because of noise limitations. Air ducting is often arranged to use the front of the machine compartment for entrance and exit of air. This makes the cooling air system largely independent of the location of the refrigerator and allows built-in applications.



Figure 2.14 Forced convection, plate fin-and-tube type condenser (Fin Condenser, n.d.).

For compressor cooling, the condenser may also incorporate a section where partially condensed refrigerant is routed to an oil cooling loop in the compressor. Here, liquid refrigerant, still at high pressure, absorbs heat and is re-evaporated. The vapor is then routed through the balance of the condenser, to be condensed in the normal manner.

Condenser performance may be evaluated directly on calorimeter test equipment similar to that used for compressors. However, final condenser design must be determined by performance tests on the refrigerator under a variety of operating conditions.

Generally, the most important design requirements for a condenser include sufficient heat dissipation at peak-load conditions; refrigerant holding capacity that prevents excessive pressures during pull down or in the event of a restricted or plugged capillary tube; good refrigerant drainage to minimize refrigerant trapping in the bottom of loops in low ambient, off-cycle losses, and the time required to equalize system pressures; an external surface that is easily cleaned or designed to avoid dust and lint accumulation; a configuration that provides adequate evaporation of defrost water; and an adequate safety factor against bursting.

### ***2.4.3 Evaporator***

The refrigerant undergoes various changes throughout the vapor compression cycle and it is in the evaporator where it actually produces the cooling effect. The evaporator is usually a closed insulated space where the refrigerant absorbs heat from the substance or food to be cooled (ASHRAE, 2006).

For smaller household refrigerating systems there are three types of evaporators: manual defrost evaporator, cycle defrost evaporator and frost-free evaporator.

The manual defrost evaporator is usually a box with three or four sides refrigerated. Refrigerant may be carried in tubing brazed to the walls of the box, or the walls may be constructed from double sheets of metal that are brazed or metallurgical bonded together with integral passages for the refrigerant. In this construction, the walls are usually aluminum, and special attention is required to avoid contamination of the surface with other metals that would promote galvanic corrosion and configurations that may be easily punctured during use

The cycle-defrost evaporator (Figure 2.15) for the fresh food compartment is designed for natural defrost operation and is characterized by its low thermal capacity. It may be either a vertical plate, usually made from bonded sheet metal with integral refrigerant passages, or a serpentine coil with or without fins. In either case, the evaporator should be located near the top of the compartment and be arranged for good water drainage during the defrost cycle. In some designs, this cooling surface is located in an air duct remote from the fresh food space, with air circulated continuously by a small fan.



Figure 2.15 Cycle defrost evaporator (Tube On Plate Evaporator, n.d.).

The frost-free evaporator (Figure 2.16) is usually a forced-air fin-and-tube arrangement designed to minimize frost accumulation, which tends to be relatively rapid in a single-evaporator system. The coil is usually arranged for airflow parallel to the fins' long dimension.

Fins may be more widely spaced at the air inlet to provide for preferential frost collection and to minimize its air restriction effects. All surfaces must be heated adequately during defrost to ensure complete defrosting, and provision must be made for draining and evaporating the defrost water outside the food storage spaces. Some more efficient designs of new evaporators' types are now commonly used in the industry. They are made of aluminum with continuous rectangular fins; fin layers are press-fitted onto the serpentine bent evaporator tube. These evaporators work in counter/parallel/cross flow configuration.

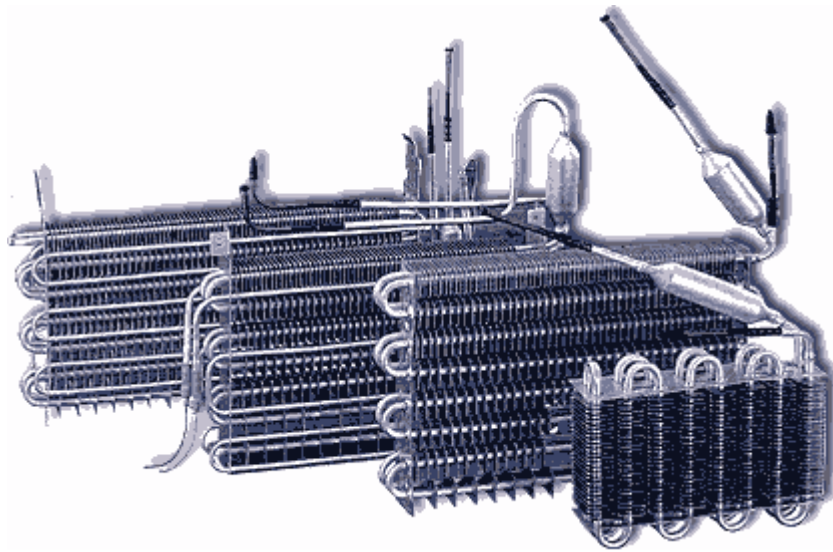


Figure 2.16 Frost-free evaporator (Fin Evaporator, n.d.).

#### ***2.4.4 Capillary Tube (Expansion Valve)***

The most commonly used refrigerant metering device (expansion valve) is the capillary tube (Figure 2.17), a small-bore tube connecting the outlet of the condenser to the inlet of the evaporator. The regulating effect of this simple control device is based on the principle that a given mass of liquid passes through a capillary more readily than the same mass of gas at the same pressure. Thus, if uncondensed refrigerant vapor enters the capillary, mass flow is reduced, giving the refrigerant more cooling time in the condenser. On the other hand, if liquid refrigerant tends to back up in the condenser, the condensing temperature and pressure rise, resulting in an increased mass flow of refrigerant. Under normal operating conditions, a capillary tube gives good performance and efficiency. Under extreme conditions, the capillary either passes considerable uncondensed gas or backs liquid refrigerant well up into the condenser (ASHRAE, 2006).

A capillary tube has the advantage of extreme simplicity and no moving parts. It also lends itself well to being soldered to the suction line for heat exchange purposes. This positioning prevents sweating of the otherwise cold suction line and increases refrigerating capacity and efficiency.



Figure 2.17 Capillary tube (Refrigerator Capillary Tube, n.d.).

Another advantage is that pressure equalizes throughout the system during the off cycle and reduces the starting torque required of the compressor motor. The capillary is the narrowest passage in the refrigerant system and the place where low temperature first occurs. For that reason, a combination strainer-drier is usually located directly ahead of the capillary to prevent it from being plugged by ice or any foreign material circulating through the system.

#### ***2.4.5 Refrigerants***

Refrigerants are the working fluids in refrigeration and heat-pumping systems. They absorb heat from one area, such as an air-conditioned space, and reject it into another, such as outdoors, usually through evaporation and condensation. These phase changes occur both in absorption and mechanical vapor compression systems, but not in systems operating on a gas cycle using a fluid such as air. The design of the refrigeration equipment depends strongly on the properties of the selected refrigerant (ASHRAE, 2006).

Refrigerant selection involves compromises between conflicting desirable thermo physical properties. A refrigerant must satisfy many requirements, some of which do not directly relate to its ability to transfer heat. Chemical stability under conditions of

use is an essential characteristic. Safety codes may require a nonflammable refrigerant of low toxicity for some applications. Cost, availability, efficiency, and compatibility with compressor lubricants and equipment materials are other concerns.

Primary refrigerants can be classified into the following five main groups. Halocarbons, Hydrocarbons (HCs), Inorganic compounds, Azeotropic mixtures, Nonazeotropic mixtures. For domestic refrigerators, R-600 (n-butane) and R134a (nonazeotropic mixture) are suitable as refrigerants can be used

Nonazeotropic mixture is a fluid consisting of multiple components of different volatiles that, when used in refrigeration cycles, change composition during evaporation (boiling) or condensation. Recently, nonazeotropic mixtures have been called zeotropic mixtures or blends. The application of nonazeotropic mixtures as refrigerants in refrigeration systems has been proposed since the beginning of the twentieth century. A great deal of research on these systems with nonazeotropic mixtures and on their thermo physical properties has been done since that time. Great interest has been shown in nonazeotropic mixtures, especially for heat pumps, because their adaptable composition offers a new dimension in the layout and design of vapor-compression systems. Much work has been done since the first proposal to use these fluids in heat pumps. Through the energy crises in the 1970s, nonazeotropic mixtures became more attractive in research and development on advanced vapor-compression heat pump systems (Dincer & Kanoglu, 2010).



# CHAPTER THREE

## FAN

Fans are also important part of refrigerators that are mainly used to transfer the air from evaporator to the compartments of No\_Frost models. They circulate the air for distribution in the compartments of Static models and increase the convection on the surface of evaporator.

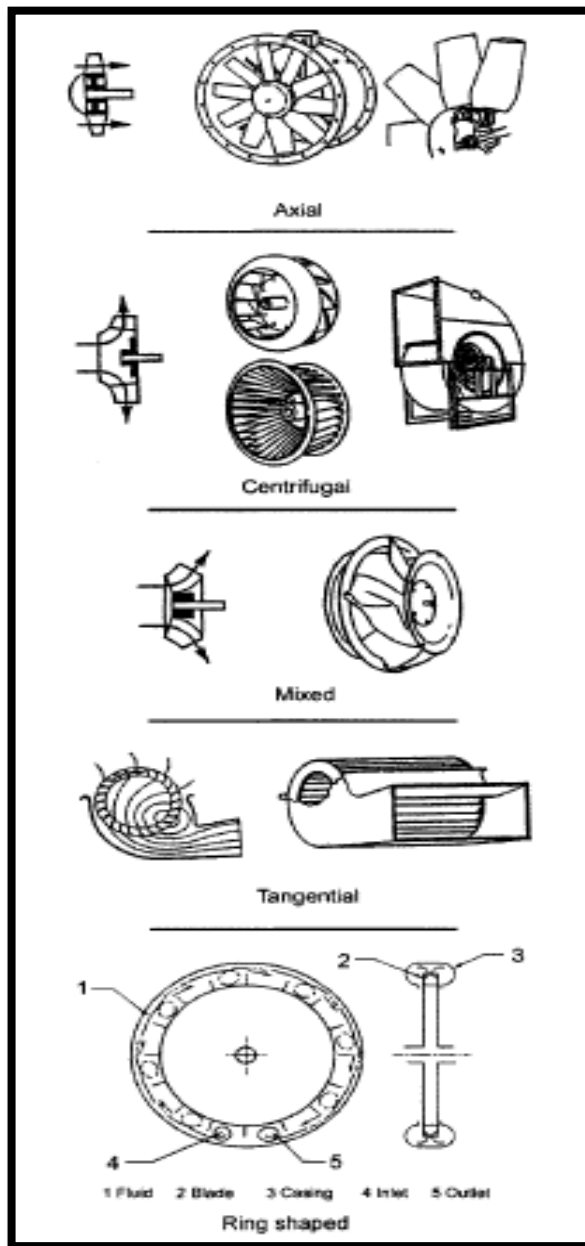


Figure 3.1 The five main fan types (Cory, 2005).



We may identify five generically different types (Figure 3.1) characterized by their impellers and the flow through them.

Propeller or axial flow where the effective movement of the air is straight through the impeller at a constant distance from its axis. The major component of blade force on the air is directed axially from the inlet to outlet side, the resultant pressure rise being due to this blade action. There is also, of course, a tangential component which is a reaction to the driving torque and the air, therefore also spins around the impeller axis. Suitable for high flow rate to pressure ratios.

Centrifugal or radial flow where the air enters the impeller axially and, turning a right angle, progresses radially outward through the blades. As the blade force is tangential, the air tends to spin with these blades. The centrifugal force resulting from the spin with these blades. The centrifugal force resulting from the spin is thus in line with the radial flow of the air, and this is the main cause of the rise in pressure. According to the blade inclination or curvature, there may also be an incremental pressure rise due to the blade action. Suitable for a low flow rate to pressure ratio.

Mixed or compound flow where the air enters axially but is discharged at an angle between say  $30^\circ$  and  $80^\circ$ . The impeller blading extends over curved part of the flow path, the blade force having a component in the discharge direction as well as the tangential component. The pressure rise is thus due to both blade and centrifugal action. Intermediate in flow rate and pressure rise between the centrifugal and axial.

Tangential or cross flow in which a vortex is formed and maintained by the blade forces and has its axis parallel to the shaft, near to a point on the impeller circumference. The outer part of this vortex air is “peeled” off and discharge through an outlet diffuser. Whilst similar in appearance to a centrifugal impeller, the action is completely different, an equal volume of air joining the inward flowing side of vortex. Thus air has to traverse the blade passages twice. Suitable for very high flow rates against minimal resistance.

Ring-shaped in which the circulation of air or gas in a toric casing is helicoidal. The rotation of the impeller, which contains a number of blades, crates a helicoidal trajectory which intercepted by one or more blade, depending on the flow rate. The impeller transfers energy to the air or gas and is usually used for very low flow rates. (Cory, 2005)

### 3.1 Types of Fans.

Apart from the effects of varying blade widths and inlet areas, other differences in fan characteristics are attributable to differences in blade shape. The diagrams are included to show the impeller configuration and typical characteristic curves are also included.

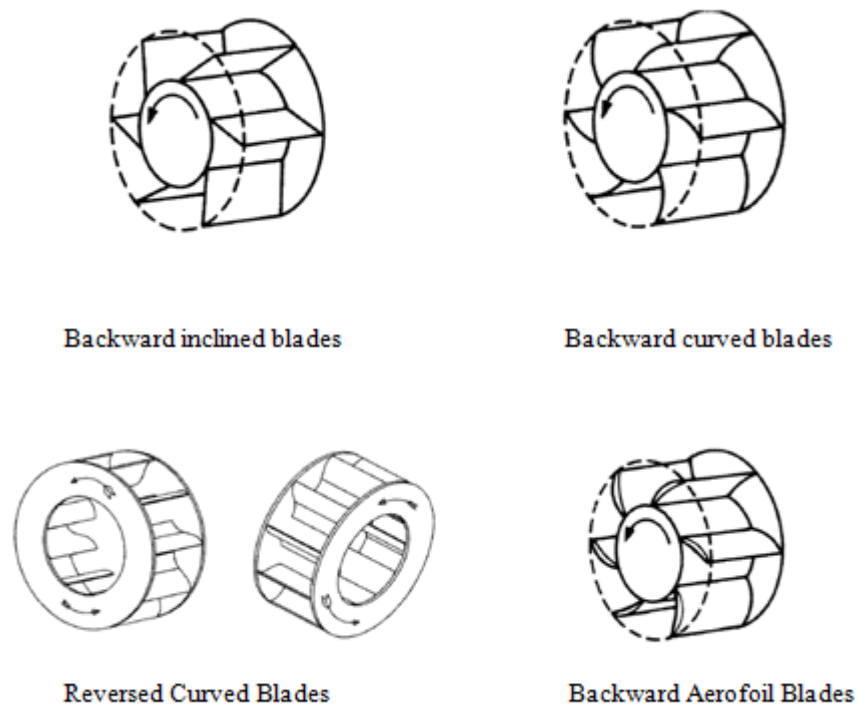


Figure 3.2 Types of fan impellers\_1 (Cory, 2005).

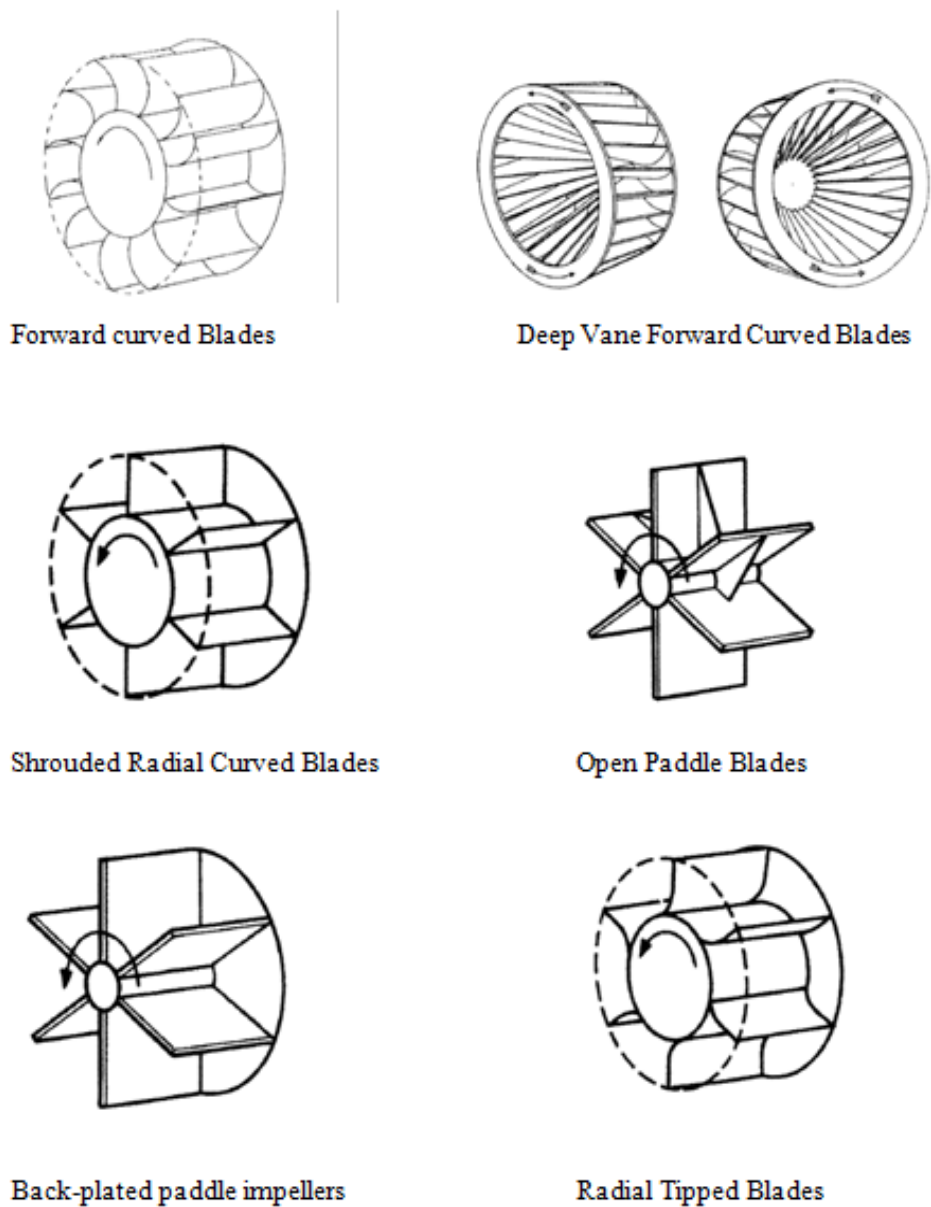


Figure 3.3 Types of fan impellers\_2 (Cory, 2005).

### ***3.1.1 Backward Curved Blades.***

These impellers are shown in Figure 3.2 and 3.3 and are preferred for certain applications where there may be disadvantages in the use of the backward inclined type. Due to the curvature, the blade angle at inlet can be made steeper for a given outlet angle. This generally enables shock losses to be kept low, whilst the curvature itself develops such fans with a pressure curve continually rising zero flow.

They can be extremely stable, with none of the “bumps” in their curves found with other types, and most suitable for operation in parallel on multi-fan plants. With the special blade curvatures now used, efficiencies exceed 82% static, approaching those attained by aerofoil bladed fans.

The steeper inlet angle also results in a stronger blade, which can rotate at higher speeds. This is offset to a large extent however, by the need to run at higher speeds for a given duty as compared with the backward inclined type. They are also more expensive as, unless complex press tools are used to “stretch” the metal, the blades cannot be flanged for riveting or spot welding and have to be arc welded in position.

The curvature of backward curved blades (concave on the underside of the blades) is inclined to encourage the build-up of dust. As the impeller in its rotation tends to develop a positive pressure on the working convex face of the blade and negative effect on the underside, dust can lodge within the camber. This becomes more pronounced on the narrowest fans where the camber is substantial and the chord is very much shorter than the developed blade length. The wider units have less curvature, although the effects are offset by the shallow outlet angles.

Generally backward curved impellers are not so suitable for high temperature operation, as differential expansion between blades and shrouds can be severe inducing additional stresses. Gas temperatures should therefore be limited to 350°C. Other advantages are the same as those of the backward include type, including a relatively steep pressure characteristic and non-overloading power curve.

### **3.2 Centrifugal Fan Mechanism.**

We shall consider firstly an ideal impeller with backward-curved blades. An ideal impeller is defined as an impeller having an infinite number of blades, so that all friction loss is eliminated and the relative motion of the air will be in the same direction as the actual blade. Furthermore, the thickness of the blades is considered to be infinitely small. At the point of entry indicated by diameter  $d_1$  the angle of the

blade to the tangent of the circumference is  $\beta_1$ , while at the point of discharge the corresponding angle is  $\beta_2$ .

It's assumed that the impeller revolves with a peripheral velocity and that the air enters the impeller in a radial direction, so that its entry into the blade passages is tangential to their direction. This type of air entry is called shock-free.

In actual cases under consideration air does not enter in a truly radial direction but at an angle  $\alpha_1$  to the circumference, as seen by a standing observer, due to the pre-rotation imposed upon the air in the direction of the rotary movement of the impeller.

Figure 1.22 shows typical velocity diagrams for entry and exit with designations customarily employed in turbine construction. The theorem of momentum in mechanics supplies us with the necessary information. When it is applied in this case, the significant point is that the resultant torque is given by the difference between the outgoing and incoming moments of momentums. Consideration the torque expressed by  $q c_u r_s$  where  $q$  is the mass flow per second through a circular disc,  $c_u$  is the circumferential or peripheral velocity of the air and  $r$  is the radius. Thus, we can write the equation below. In this equation,  $q$  is taken outside because it has a constant value at inlet and outlet (Eck, 1975).

$$M = q (r_2 c_{2u} - r_1 c_{1u}) \quad (3.1)$$

Energy transformation is considered as being perfect and therefore losses have not been considered, so that the energy supplied is the same as the energy at discharge. If one considers the mass flow per second  $q$  to consist of solid particles which are raised through a height  $H$  in one second, the rate of working or power due to the displacement is given by "H.q.g".

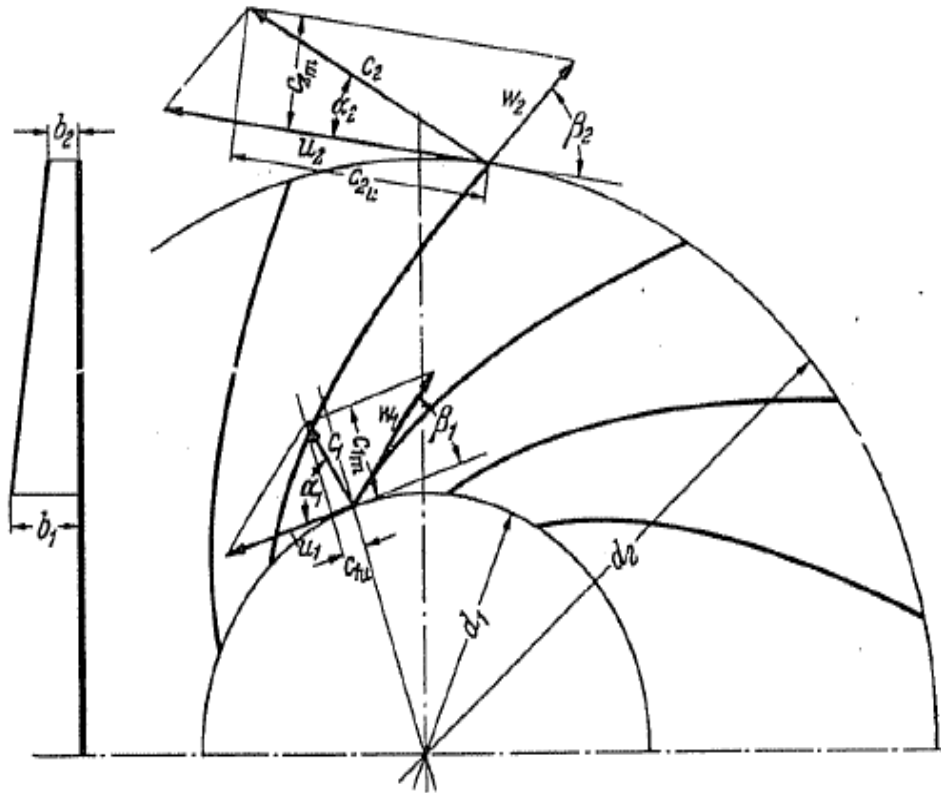


Figure 3.4 Impeller with backward-curved blades and other details (Eck, 1975).

If the impeller rotates with an angular velocity  $\omega$  radians/sec, then the power is  $L=M\omega$ . We write

$$L = M\omega = H_{th\infty}qg = q\omega[r_2c_{2u} - r_1c_{1u}] = q[u_2c_{2u} - u_1c_{1u}], \quad (3.2)$$

and from this,

$$H_{th\infty} = \frac{1}{g} [u_2c_{2u} - u_1c_{1u}], \quad (3.3)$$

by radial entry ( $c_{1u} = 0$ ), therefore,

$$M = q r_2 c_{2u} \quad H_{th\infty} = \frac{1}{g} [u_2 c_{2u}] \quad (3.4)$$

In the case of fluids and gases, the meaning of the term “height of lift” is identical with “pressure head”; its relation to pressure in excess of atmospheric is given by

$$\Delta p = \gamma H \quad (3.5)$$

( $\gamma$  density of a liquid or gas).

In fan design we input the pressure in excess of atmospheric  $\Delta p$  in place of  $H$ , so that we write

$$\Delta p_{th\infty} = \frac{\gamma}{g} [u_2 c_{2u} - u_1 c_{1u}] = q [u_2 c_{2u} - u_1 c_{1u}], \quad (3.6)$$

$$\Delta p_{th\infty} = q [u_2 c_{2u}] \quad (\text{radial entry}) \quad (3.7)$$

In the practice of fan design, density is the only physical property of gases and vapours that receives attention. The density  $\gamma$  is derived from the general gas equation;

$$p\vartheta = p/\gamma = RT \quad \text{or} \quad \gamma = \frac{p}{RT} \quad (3.8)$$

Atmospheric air is almost always moist and one should remember that moist air is always lighter than dry air. In the case of higher temperatures to which moist air might be subjected, the decrease of density becomes important. Figure 3.5 shows the reduction of density for air of 50% and 100% humidity in relation to the temperature.

In general, when air enters an impeller it has no peripheral component. Such a component must first be produced through inlet vanes. If these vanes are not available then the air enters radially and according to Equation 3.8.

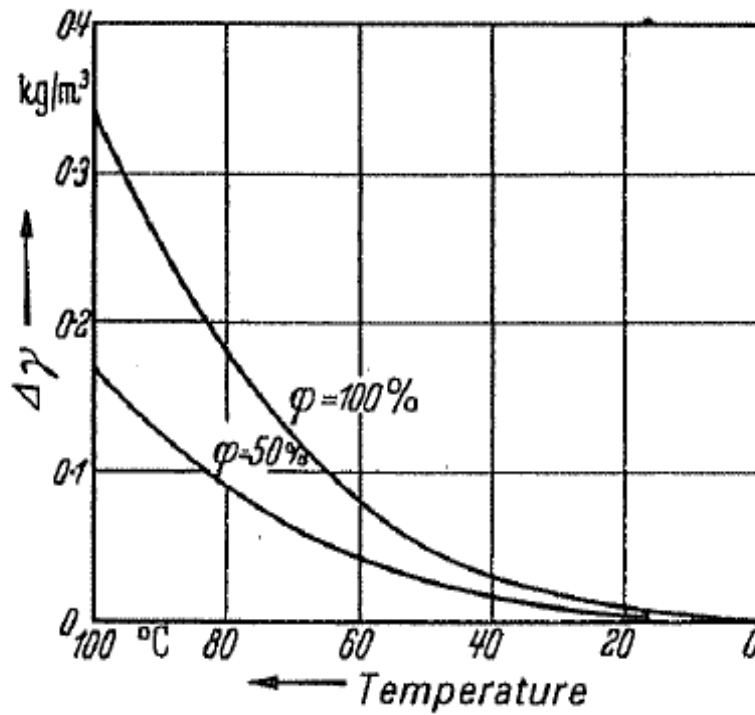


Figure 3.5 Percentage decrease of density of moist air with decreasing temperature (Eck, 1975).

A further simplification is possible. If one substitutes a coefficient  $\tau$  for the ratio  $c_{2u}/u_2$ , pheral component  $u_2$ ,

$$\Delta p_{th\infty} = \frac{\gamma}{g} u_2^2 \frac{c_{2u}}{u_2} = \frac{\gamma}{g} u_2^2 \tau \quad (3.9)$$

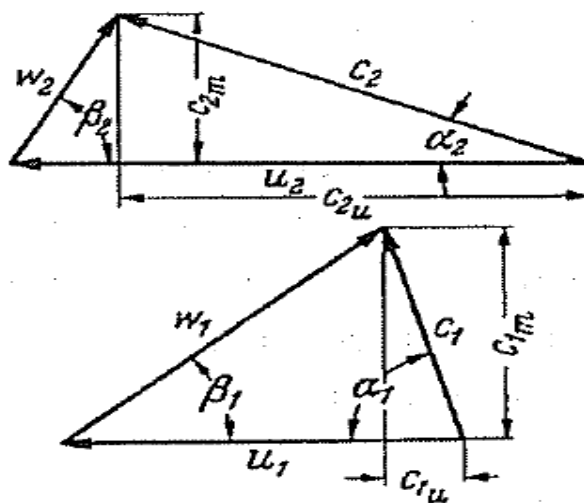


Figure 3.6 Velocity triangles for backward-curved blades (Eck, 1975).



The dimensionless coefficient  $\tau$  is dependent only on the angle of the velocity triangle. From Figure 3.6 through the application of the sine-rule we obtain  $c_2 = u_2 [\sin \beta_2 / \sin(\alpha_2 + \beta_2)]$ ; this is introduced in  $c_{2u} = c_2 \cos \alpha_2 = \frac{\sin \beta_2 \cos \alpha_2}{\sin(\alpha_2 + \beta_2)} u_2$ , so we get,

$$\tau = \frac{c_{2u}}{u_2} = \frac{\sin \beta_2 \cos \alpha_2}{\sin \alpha_2 \cos \beta_2 + \cos \alpha_2 \sin \beta_2} = \frac{\tan \beta_2}{\tan \alpha_2 + \tan \beta_2} \quad (3.10)$$

therefore  $\tau$  represents a function of the blade angle  $\beta_2$  and the outlet angle  $\alpha_2$  of the absolute velocity.

In Figure 3.7 the value of  $\tau = \frac{c_{2u}}{u_2}$  is shown as a function of  $\alpha_2$  for different angles of  $\beta_2$ . With the use of Figure 3.7, if the peripheral velocity is given, the increase in pressure of a frictionless impeller having an infinite number of blades can be determined.

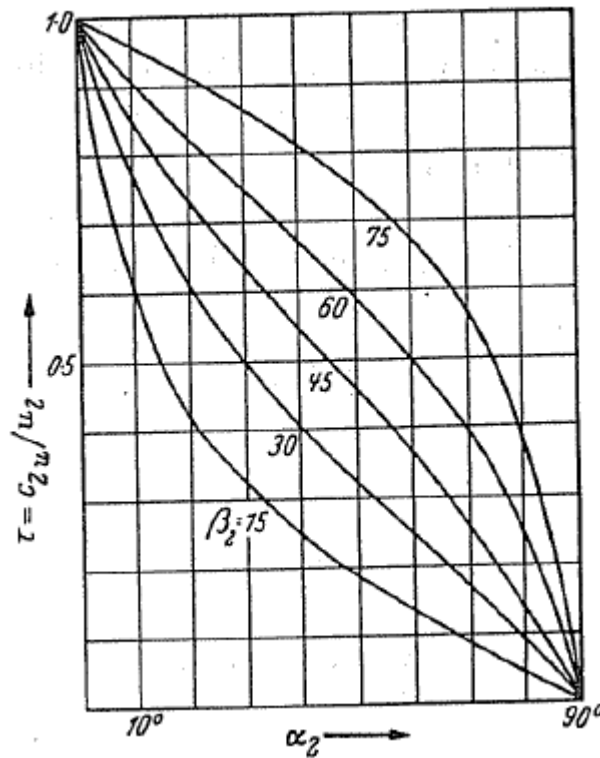


Figure 3.7  $c_{2u}$  divided by  $u_2$  plotted against  $\alpha_2$  (Eck, 1975).

## **CHAPTER FOUR**

### **EXPERIMENTAL STUDY**

In this chapter, particle image velocimetry (PIV) which is a flow visualization method will be explained in details. According to this method, the velocity profile will be visualized through the duct of a centrifugal fan which is generally mounted on the No-Frost refrigerator models. In the following parts, measured velocity profile results will be transferred to the numerical study as an initial condition. This study provides us with an opportunity to compare the numerical and the experimental studies.

#### **4.1 Methodology of Particle Image Velocimetry (PIV)**

PIV method is based on observe and visualize the path line of fluid to determine the flow characteristic. Visualization of fluid is also possible with small reflexivity particles that adrift throughout the flow and can be easily viewed.

Generally a laser is used to create a light sheet on the interested area to illuminate these particles clearly. PIV measurement is possible on the plane that was created by a high power light source (generally a laser). One camera is placed in front of light sheet and an extra camera is placed with an angle to obtain third dimension during the measurements.

Because of high shutter speed ( $1/6250000$ ), really small amount of light could reflect and get inside the camera. Therefore high power light source is an obligatory to capture these images clearly. These specific equipments are also devices to determine the displacement of small particles that adrift through the flow.

Particles' velocity vectors on the light sheet plane are calculated from the succession of the images that are taken rapidly on short notice with a computer program. Additionally, the second angled camera is enabled the third axis of the particles' displacements.

### 4.1.1 Equipment and Apparatus of PIV

As it is also mentioned in the previous parts of this study conventional PIV setup consist of five components. These components are the laser (light source), camera and lens setup (imaging equipment), synchronizer, fog generator (seeding device) and analysis computer. Although these components exist in every PIV setup, they can have different specs according to the system that is needed to investigate. Table 4.1 shows the components of the present PIV setup that is used in this study and Figure 4.1

Table 4.1 Specifications of the PIV system components.

Component	Specifications
1) <b>Laser</b>	135mJ, 15Fps double pulse ND: Yag Laser
2) <b>Camera &amp; Lens</b>	Flow Sence Mark2, 4 MPx, square sensor camera. 60mm f 2 Zeiss Planar Macro Lens
3) <b>Synchronizer</b>	Dantec Dynamics Synchronizer Box
4) <b>Fog Generator</b>	Safex fog generator, with extra clean fog fluid
5) <b>Computer</b>	Dell T7500 work station, 12 GB ram, Raid 0

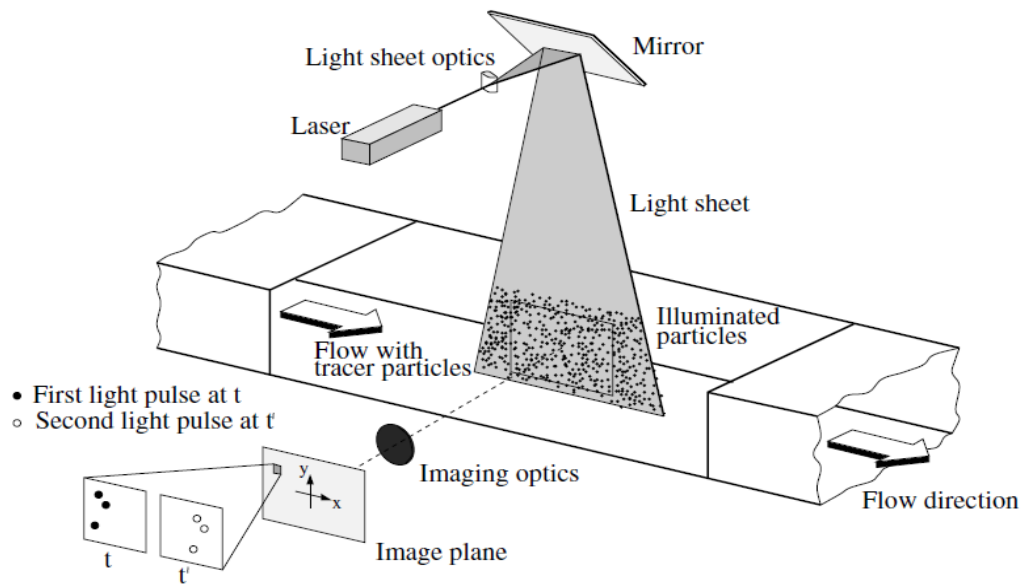


Figure 4.1 Experimental arrangement of PIV in a wind tunnel (Raffel, Willert, Wereley & Kompenhans, 2007).

#### 4.1.1.1 Seeding Particles

Depending on the fluid, the particles should be followed the flow path perfectly to succeed accurate solutions. The particle choice is dependent on the specification of the fluid.

Not only the particles should be small enough (approximately 10 to 100 micrometers) to follow the flow, but also large enough to reflect on and be scatter towards the cameras.

Critical point about seeding particles, if they are accordant with fluid under investigation or not. PIV analysis accuracy is directly related to match the fluid and particle properties reasonably well. Another important case is refractive index for seeding particles. They must be able to reflect inside the fluid with the laser sheet and be scattered towards the camera.

The particles dimensions are around 10 to 100 micrometers as not only be small enough to accurately follow the flow, but also be large enough to scatter and visualize accurately within the laser sheet plane.

Distributions of particles are also important to have successful results from PIV analysis. It's possible to use cross correlation to measure the displacement with mid-density particles. Different densities of particle can be seen in Figure 4.2.

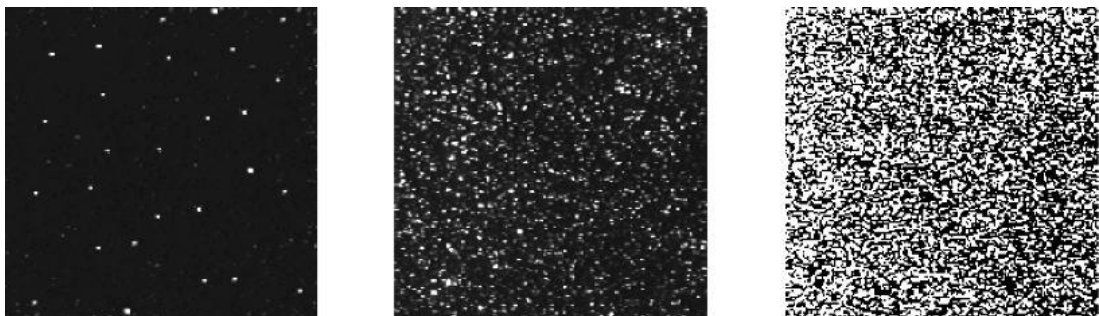


Figure 4.2 Densities of particle distribution (Raffael, Willert, Wereley & Kompenhans, 2007).

#### 4.1.1.2 Cameras and Lenses

Generally two exposure of laser sheet frame were captured on the same frame. Autocorrelation process which is not clear enough to realize the particle between first and second pulse was used to determine the flow for analysis. Faster digital cameras can capture two frames at high speed and using CCD chips. Therefore each exposure could be isolated on its own frame which is more accurate than cross-correlation analysis. The shot must be transferred to the computer before another shot will be taken. High speed CCD cameras have larger limitation about pair of shots than typical cameras.

The lenses direct all the light to a point. The rays that reach lens from any point on the object are effectively parallel. As before the images is formed close to the lens, inverted, laterally reversed and real. The image plane in which this image is formed is termed the principal focal plane (F). For a flat distant object and an 'ideal' lens, every image point lies in this plane. The point of intersection of the focal plane and the optical axis is termed the rear principal focus (or simply the focus) of the lens, and the distance from this point to the lens is termed the focal length (f) of the lens (Jacob, Ray, Attridge & Axford, 2000). The schematic of this system can be seen in Figure 4.3.

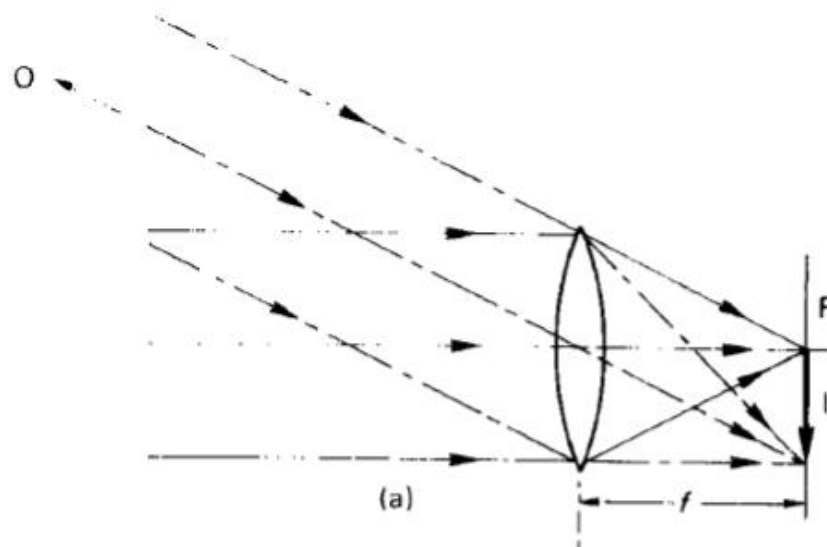


Figure 4.3 The schematic of lens and its focal plane (Jacob, Ray, Attridge & Axford, 2000).

Lenses are classified by focal length. While greater focal length lenses are used to magnify the farther images is called telephoto lens, the opposite lenses have closer focal length is called wide angle lenses. Also a normal lens creates an image view is almost close that a human eye sees. There is a relation between focal length and angle of view that if focal length shortens, angle of view gets larger. In this study to visualize the small particles, a telephoto lens is used to have a bigger and closer objects' view.

#### *4.1.1.3 Laser and Optics*

For macro PIV setups, lasers are predominant due to their ability to produce high-power light beams with short pulse durations. This yields short exposure times for each frame. Nd: YAG lasers, commonly used in PIV setups, emit primarily at 1064 nm wavelength and its harmonics (532, 266, etc.) For safety reasons, the laser emission is typically band pass filtered to isolate the 532 nm harmonics (this is green light, the only harmonic able to be seen by naked eye). A fiber optic cable or liquid light guide might be used to direct the laser light to the experimental setup.

#### *4.1.1.4 Synchronizer*

The synchronizer that is controlled by computer organizes the timing periods of camera(s) and laser within 1 ns precision. Time between pulses of the laser shot and camera's timing are controlled in order to determine the velocity of the fluid according to PIV analysis.

#### *4.1.1.5 Analysis*

Displacement vector data is calculated for each window that are configured with correlation techniques. Therefore, difference between the physical images of each frame on the camera and the time between the laser shots is converted to a velocity data. It's possible to have a visual from PIV at least 6 particles on the same window to calculate an average.

PIV analysis accuracy is related the timing between image exposures. If images' time spacing is longer, it is hard to distinguish the particles from each other, or it takes shorter, it is hard to identify any displacement in the flow. An average displacement is about 8 pixels in order to display an ideal region of flow.

#### 4.1.2 Stereoscopic PIV Setup

There are also different types of Setup according to content of study. SPIV method is preferred in this study which sets with two cameras in order to have three dimensional velocity values on the same plane. This method also provides an advantage that two cameras prevent geometric distortion caused by the lens. Stereoscopic PIV Setup permits to determine displacement on three axis. One camera positioned in front of image and another camera viewing angles to extract the z-axis. Their focal points must be coincident on the same spot. SPIV system shows Figure 4.4

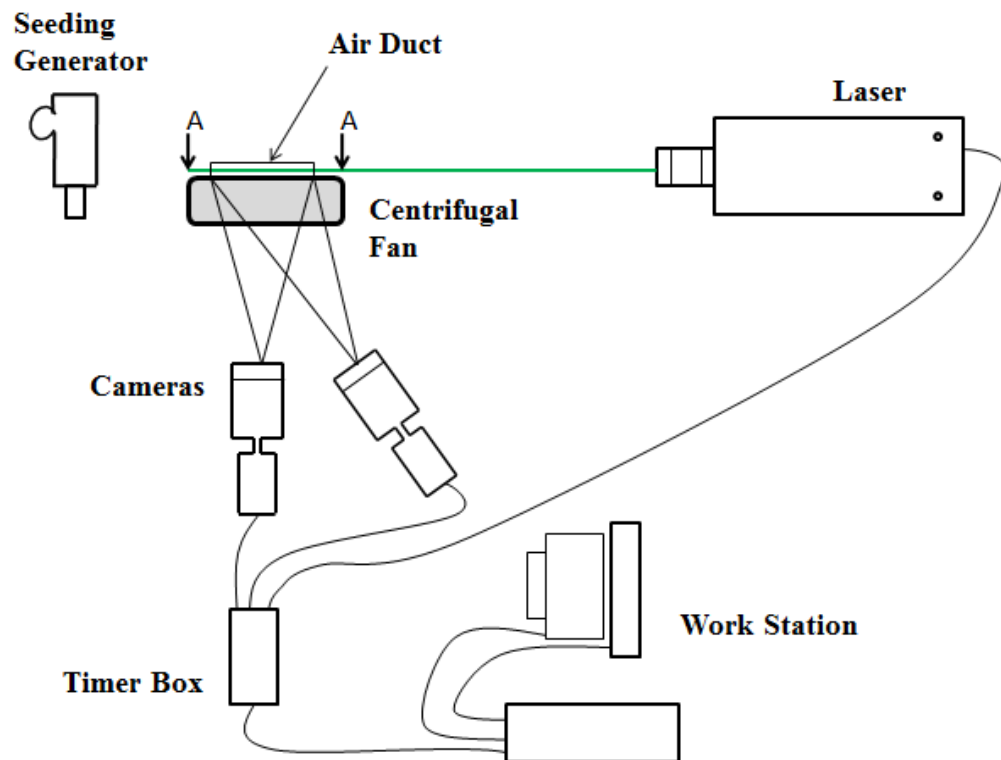


Figure 4.4 Schematic view of PIV set up components.



Figure 4.5 Calibration target and cameras (Özer, 2011).

Calibration of two cameras is critical process in system setup. Figure 4.5 shows cameras' positions which capture the images. It's also possible to have three dimensional data with two cameras which one of them is positioned with an angle and focused on the target with a perspective view. The plane where is required to scan on the fan is positioned on the calibrated plane. Data was measured from different planes to determined flow characteristic. Results are shared next chapter.

## **4.2 Results**

Firstly experimental study is performed on the full model of the fan to determine the flow characteristic at the exit region and to make verification with CFD results. Secondary experimental study is performed on cutoff model of the fan (without duct). Export data is used for numerical study of the duct as a boundary condition.

### ***4.2.1 Full Model Experiment***

Exit region of full model was divided 17 lateral planes with the help of a laser (Figure 4.6) to scanning instantaneous flow field in the downstream. The data is used to determine the exit region flow characteristic in details and validate the CFD results.



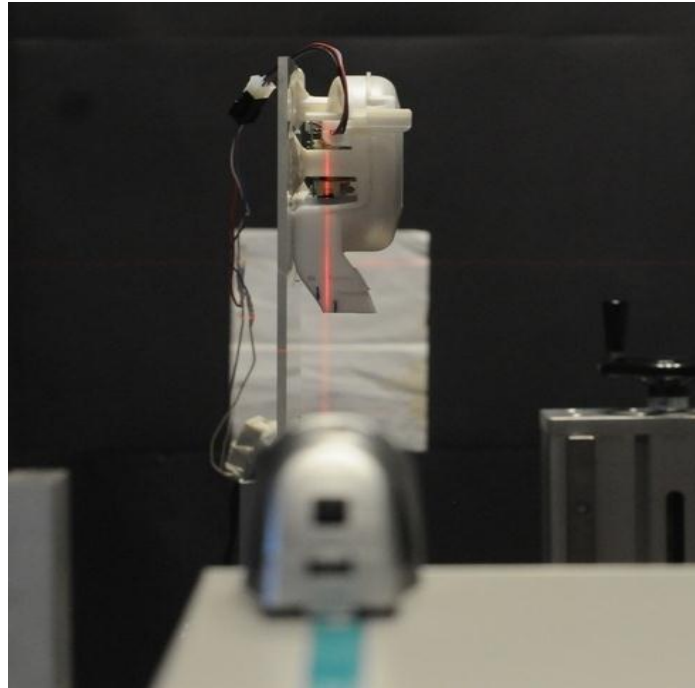


Figure 4.6 Lateral planes.

Average velocity distribution at exit region of full model is shown in Figure 4.7-8-9. Results are shared as the three dimensional planar velocity. Velocity distributions of  $V_x$  and  $V_y$  were indicated with vectors. Contours are used to define velocity through the z axis. Highest absolute velocity of 7.5m/s was pointed at right exit position and it decreases through the left side and farther away. It's obviously seen that flow direction was inclined right and positive direction on z axis. For this reason the parametric study was implement with different types of baffles that is positioned inside the duct geometry.

Results were taken 17 planes which were positioned from back at the beginning of the duct to further of the geometry. It is find unnecessary to share the plane where was at the back, because of negligible values. Plane 4, 5, 7 were taken at through the duct and plane 9, 11, 17 were positioned at the exit region of fan. These results are make us determine the flow characteristic. In the left-bottom region of Figure 4.7, the flow velocity is lower due to the lesser influence of the impellers and structure of duct. Additionally these are comparing with numerical study results next chapter.

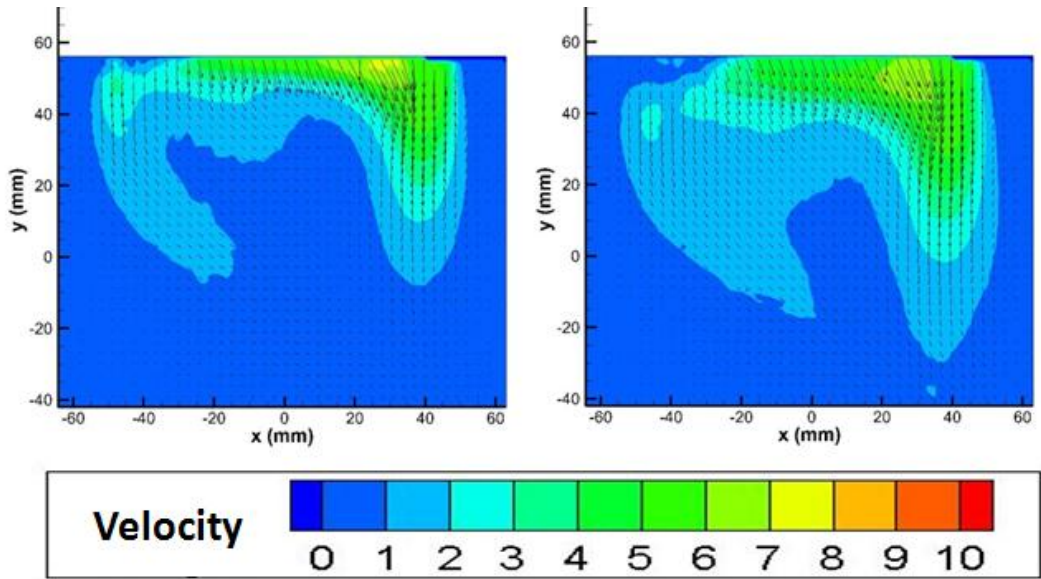


Figure 4.7 Instantaneous SPIV results on investigation plane 04-05.

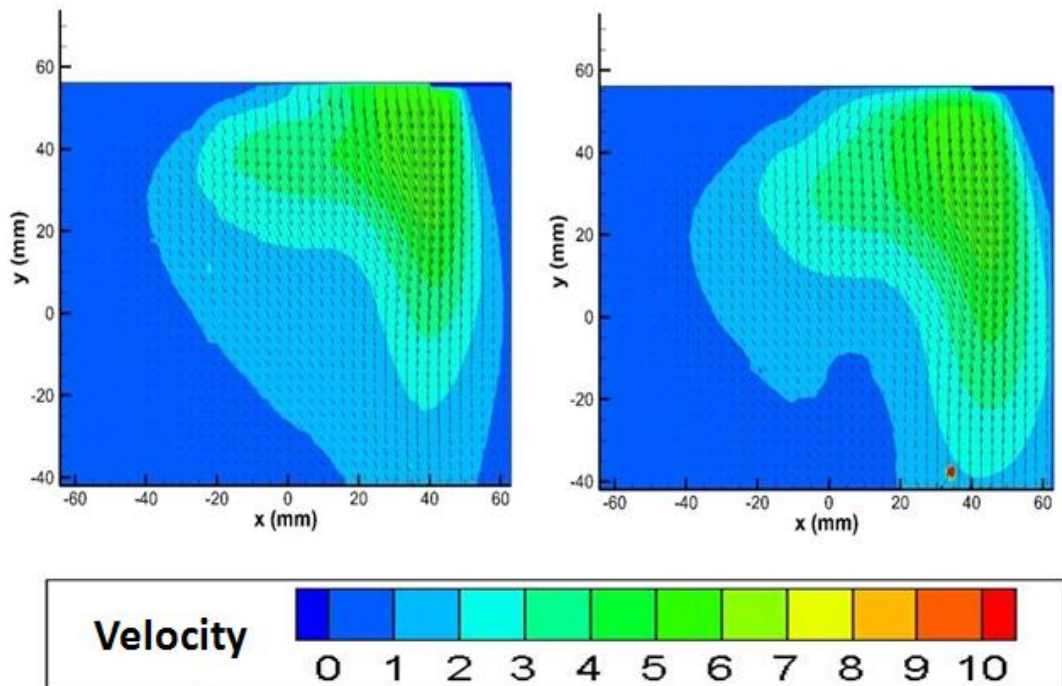


Figure 4.8 Instantaneous SPIV results on investigation plane 07-09.

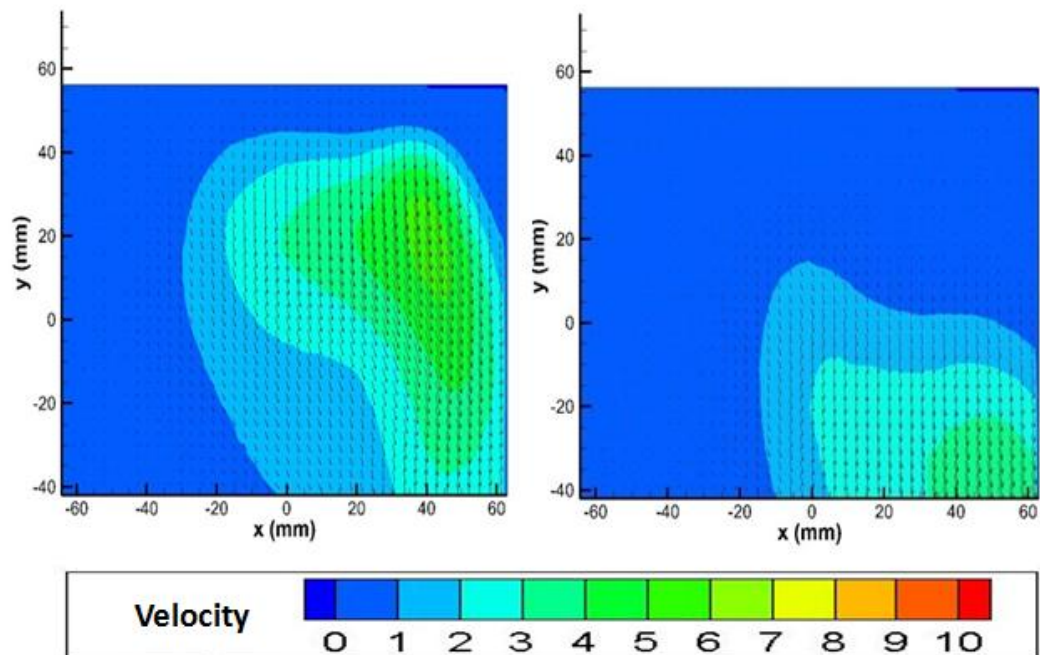


Figure 4.9 Instantaneous SPIV results on investigation plane 11-17.

#### 4.2.2 Cutoff Model Experiment

The duct is cut off in order to visualize the flow characteristic at the duct inlet region. Cutoff model is scanning on 10 different planes to export the PIV data that are used for CFD studies of duct as a boundary condition. Approximately average velocity is between 4-6m/s throughout the boundary. Because of the structure of radial fans' impellers, flow direction was inclined left side of the boundary region. Maximum vorticity of over 8m/s is observed on the right upside in the figures. Also this flow distribution satisfies the physical model that impellers rotate counterclockwise.

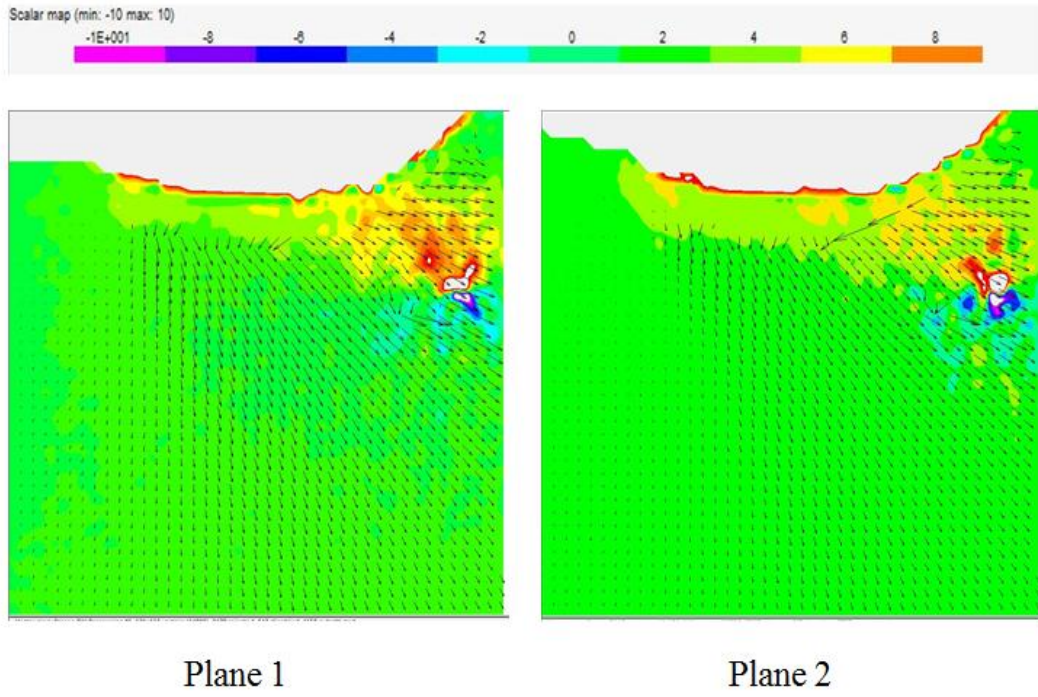


Figure 4.10 Average three dimensional velocity distribution at the boundary region on investigation plane 1-2.

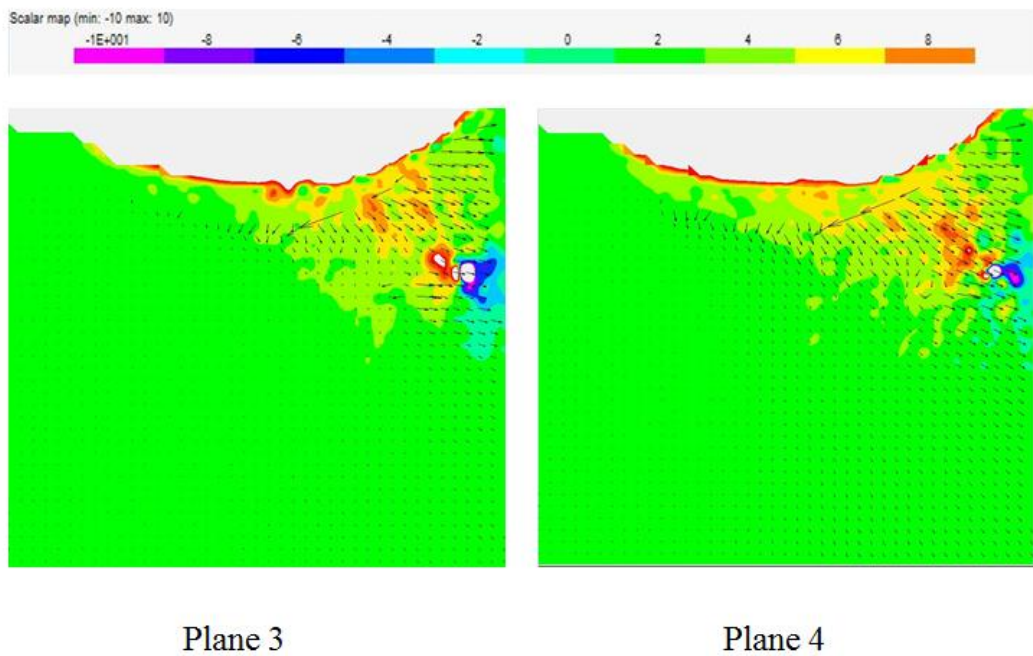
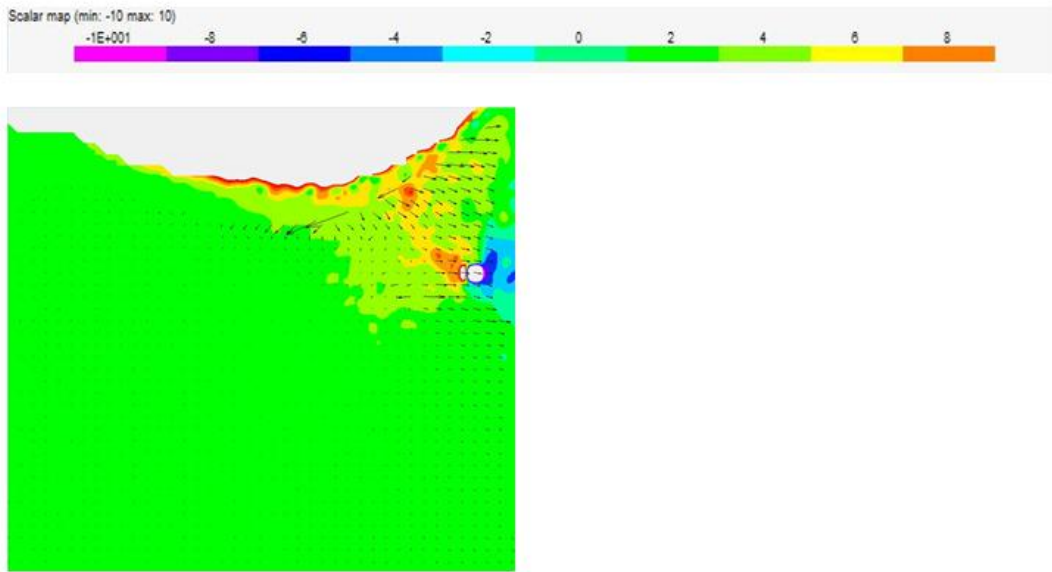


Figure 4.11 Average three dimensional velocity distribution at the boundary region on investigation plane 3-4.



Plane 5

Figure 4.12 Average three dimensional velocity distribution at the boundary region on investigation plane 5.



## CHAPTER FIVE

### NUMERICAL STUDY

Numerical study was carried out on the radial fan that was mounted on Frost\_Free models which are belongs to a commercial refrigerator producer company. The radial fan was analyzed in order to determine the distribution of velocity values and vorticity vectors inside the duct. On the other hand revision study could be started as a second step that was based on experimental study for full model. At the last step some parametric studies were implemented that was included three baffle designs. Parametric study gives an opportunity to have different design predictions' results.

#### 5.1 Methodology

Fan is mounted on the back-wall of the compartments symmetrically in order to increase the thermal convection from evaporator. Mainly purpose is not only have the maximum air flow rate, but also the linear flow at the exit region of air duct. Thereby, CFD domain includes fan's air duct and a control volume that was shown in Figure5.1. Initial velocity condition was given according to experimental studies' results which are explained previously chapter.

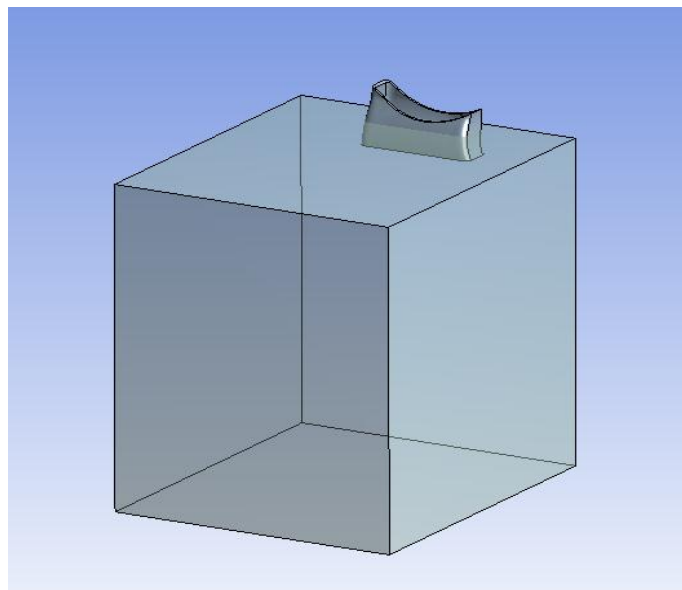


Figure 5.1 Control volume of geometry.

Mesh process and defining correct boundary conditions are most important points of computational fluid dynamics. Face size option was defined for boundary condition surface (Figure 5.2) in order to accommodate to mesh elements and nodes unless there was any missing PIV data input that should have corresponding mesh element.

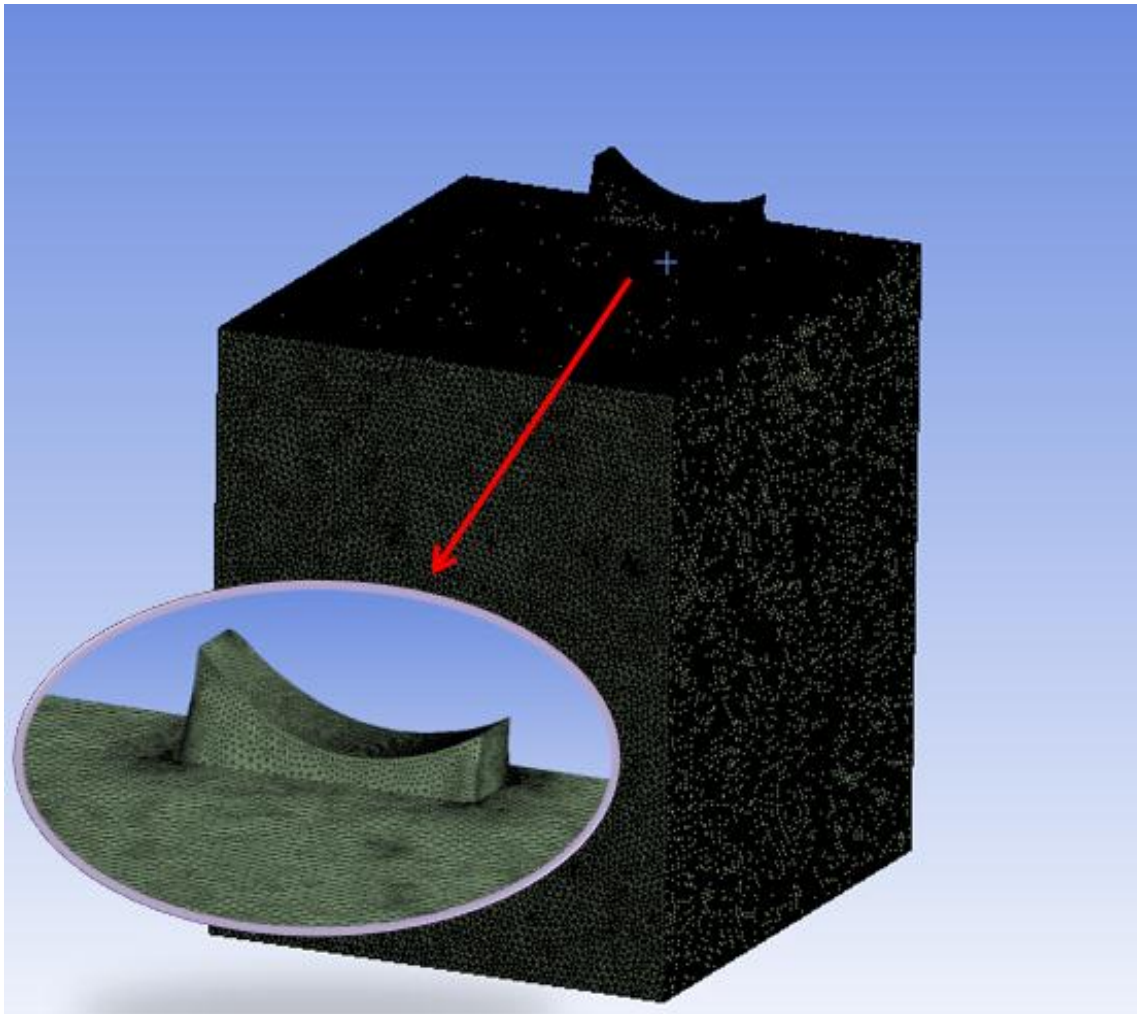


Figure 5.2 Mesh processing.

Air duct and control volume composed of 363238 nodes and 2021275 tetrahedral elements according to previously experimented studies. Mesh structure is shown in Figure 5.3 as three dimensional section from the middle of the control volume.

PIV data was converted to boundary condition format with a MATLAB code. CSV type of file was created that was involved 2821 position and velocity values on

x,y,z directions after bad vectors were determined and cleaned. The .csv file was imported as a boundary condition to the inlet surface of duct.

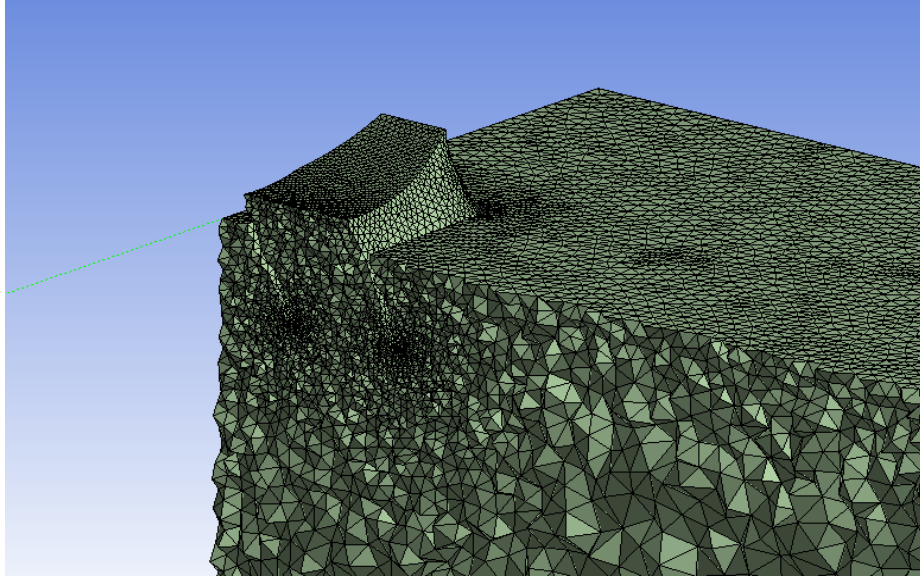


Figure 5.3 Mesh processing.

Boundary condition of control volume was given opened wall except of back-wall.and 1 atm pressure. After it was considered that there was some reverse flow vectors according to PIV result, Standard k- $\epsilon$  turbulence model was used because of its wide predictive capability on turbulence or vorticity conditions.

Three dimensional steady state analyses were preserved 300 iterations and the residuals were reached  $10 \cdot E^{-4}$  that were shown in the Figure 5.4 and 5.5. After the convergence were reach acceptable values, result was displayed according to validate for the PIV result.



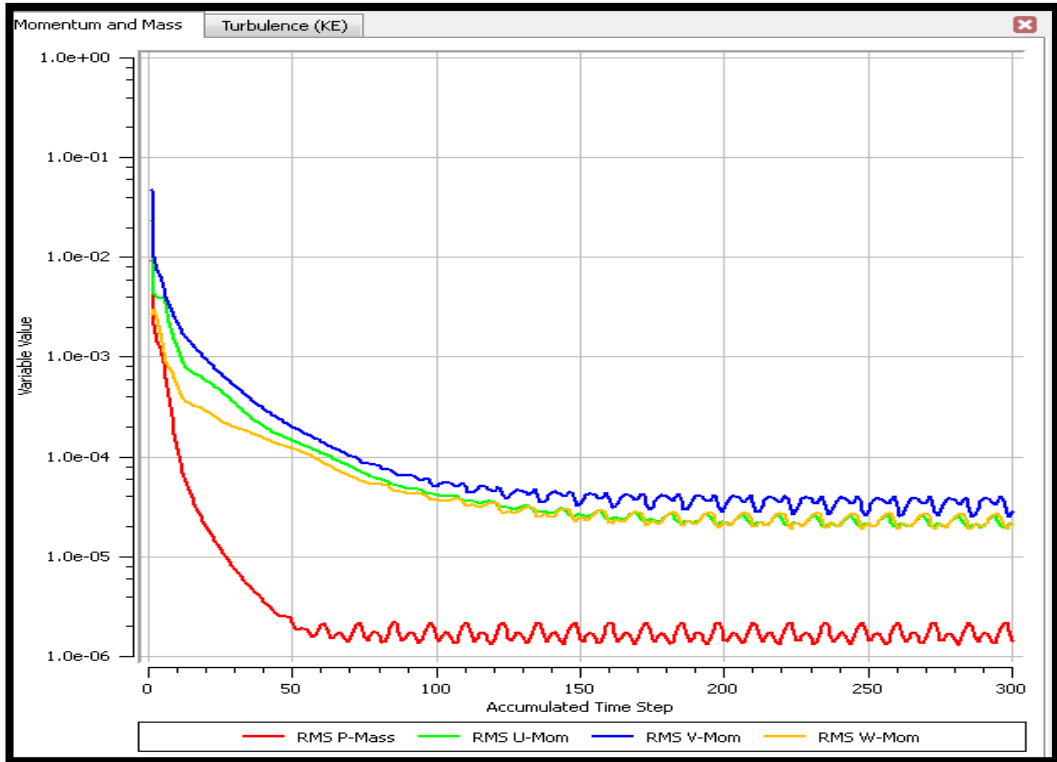


Figure 5.4 Momentum and mass residuals.

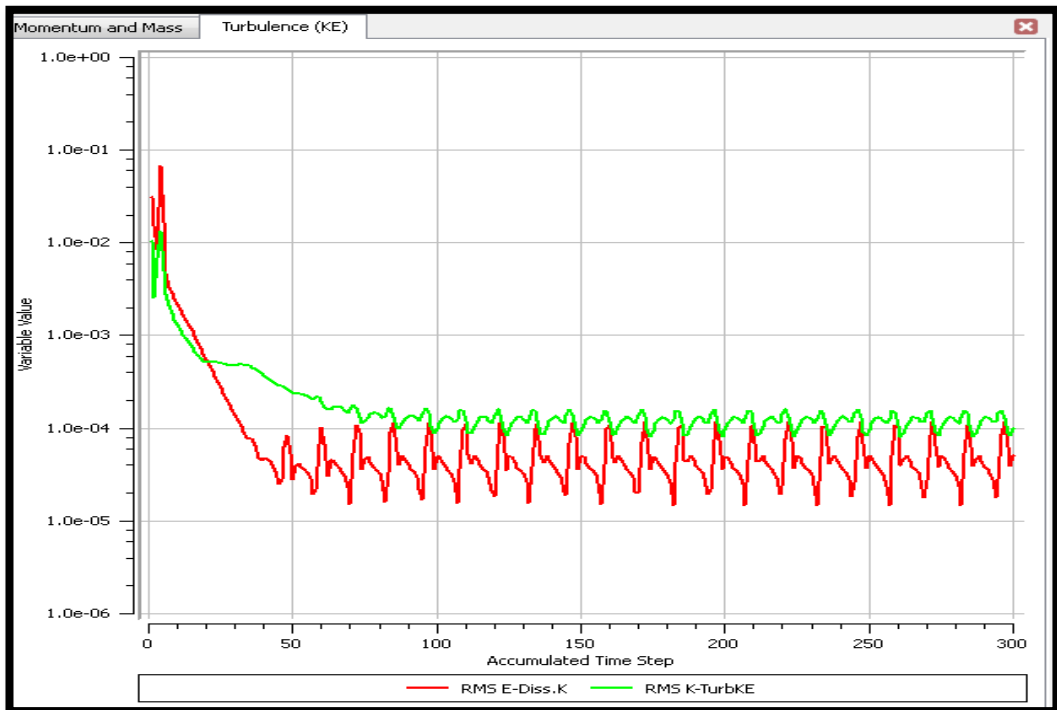


Figure 5.5 Turbulence residuals.

## 5.2 Validation & Results

PIV measurements were carried out behind the plexy glass where the fan was mounted to synchronized the PIV setup and calibrate the cameras on the target correctly. Experiment was started the steady state conditions were obtained at the ambient.

PIV result of the full model was compare with CDF study. Ensemble average flow fields are shown in Figure 5.6 and 5.7. Validation of the CFD study was evaluated by the measurement of velocity at the exit region.

Control planes were determined according to PIV image planes' coordinate. Velocity vectors' directions and values were decided to convenient due to the identical planes. Also influence areas resemble for each flow sections.

Plane 04-05-07 were taken from the outlet constrains of the duct. Basically characteristics and velocity values showed similarity in a negligible range. Plane 09-11-17 were processed from the exit region of the duct. Distributions and flow directions were in acceptable ranges according to images and values.

Distribution of velocity vectors and contours were point that the flow characteristic was inclined right side and positive z direction according to both PIV and CFD results.

According to full model results and investigation of validation, Consistency of validation results' provided us an opportunity to implement design revisions on the duct geometry. It's also possible to carry out wide range of study on different baffle designs and positions.

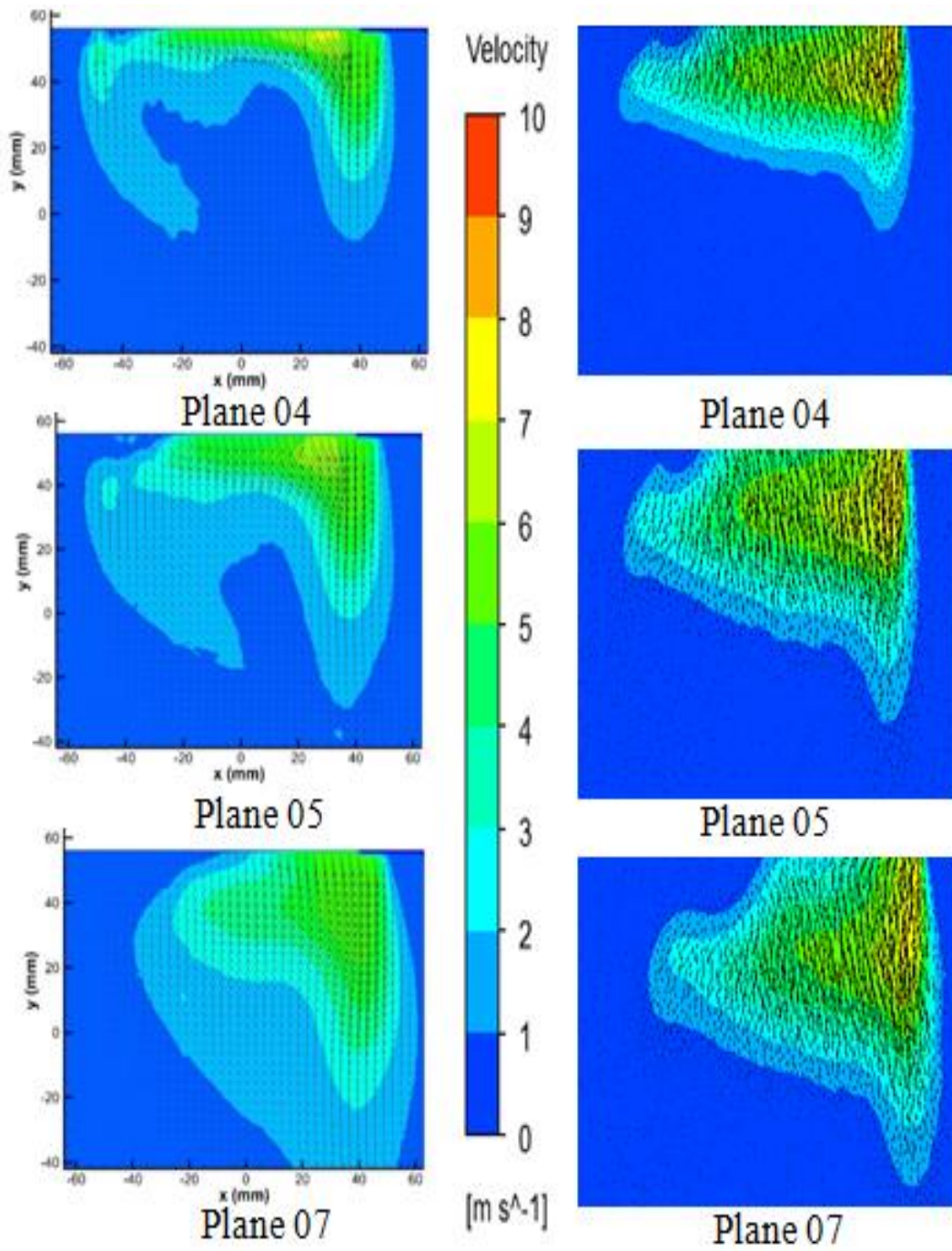


Figure 5.6 Distribution of average velocity values at the out flow section on investigation planes.

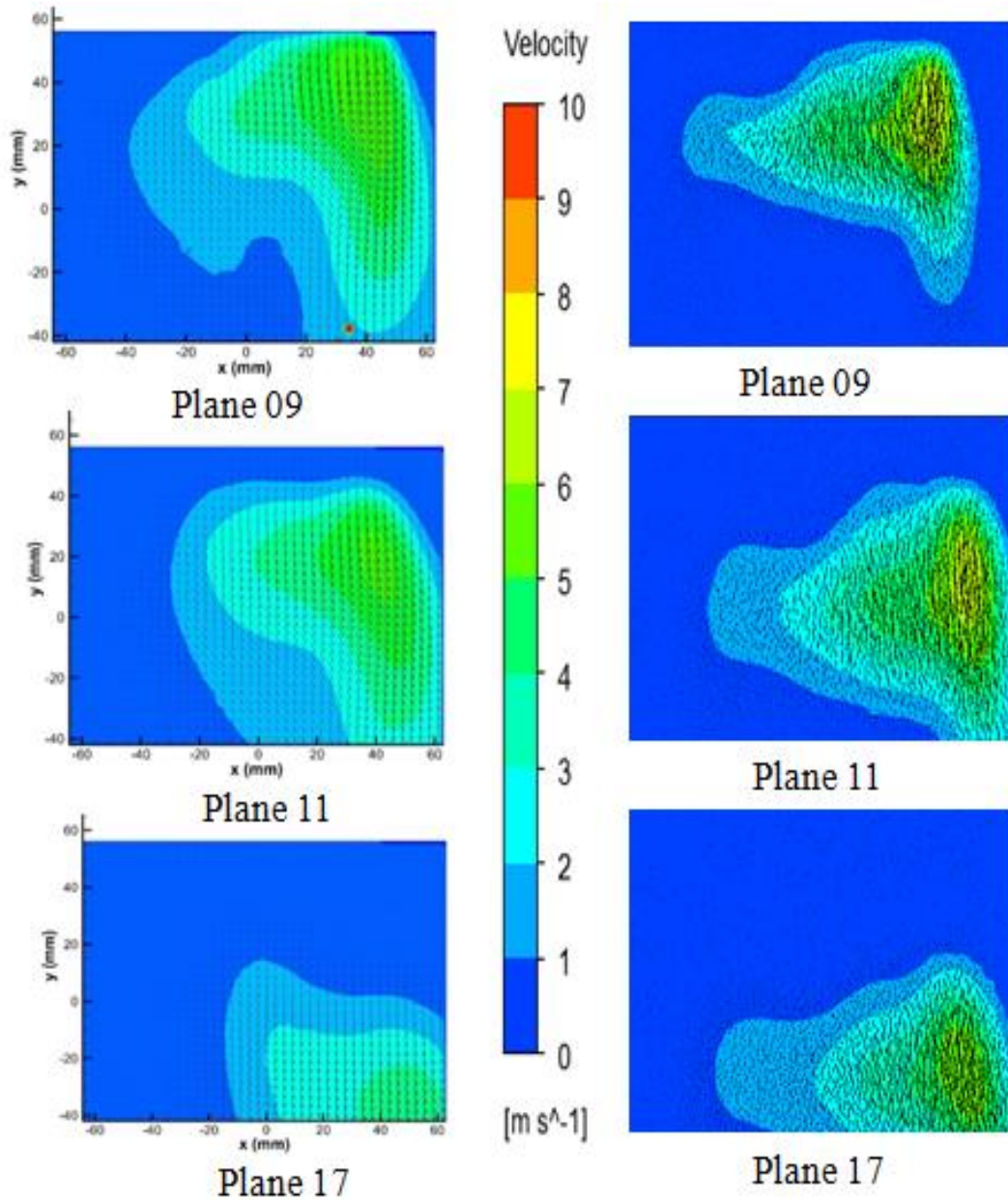


Figure 5.7 Distribution of average velocity values at the out flow section on investigation planes.

### 5.3 Parametric Study

Three different sketches were designed and subtracted from the duct air geometry inclined the direction of inlet air flow that come from impellers. Complexity of flow characteristic also was determined previously chapters. Dimensions of baffles were determined according to parametric study in order not to give a fault result for different positions under the flow phenomena.

First positions of implemented baffle types are shown in Figure 5.8. This study was consisting of three different baffle designs that were included position, angle and radius parameters. Figure 5.9, 5.10 and 5.11 summarize the results of the parameters used in the duct model for simulating the balance of exit velocity values.

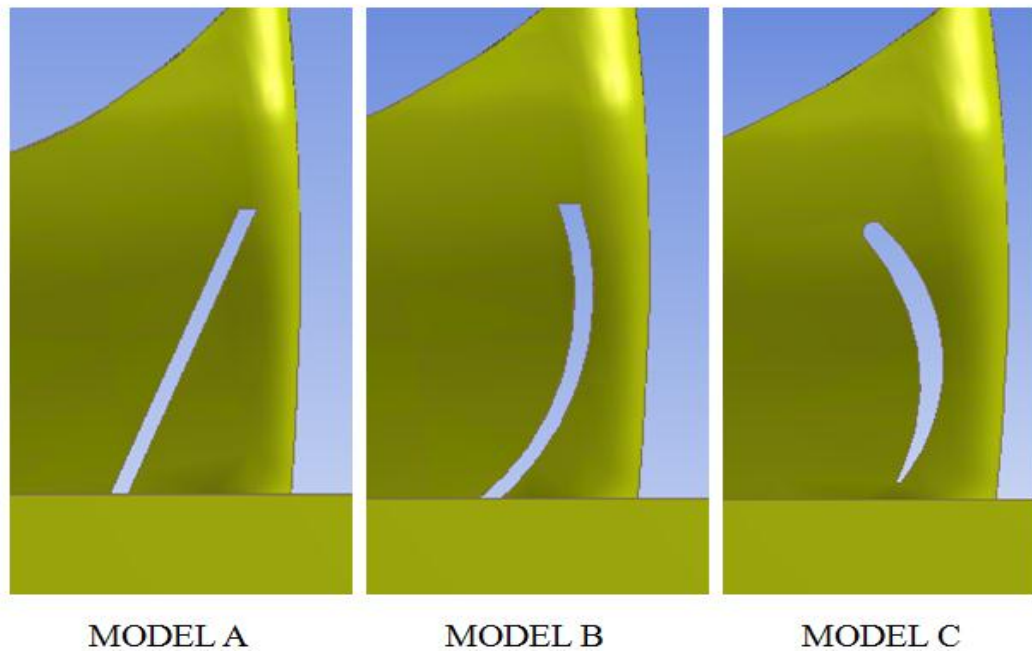


Figure 5.8 Design of baffles that are used for parametric study.

Model A was designed to determine the influence of angle parameter on the average velocity values at the out flow section. Three angles were analyzing for 10 different positions along with the duct x axis. Results are evaluated in Figure 5.9.

Sides of outlet section almost equalized between 130mm to 140mm for different angles' results. Another important point is average velocity value. Most effective result was determined as  $90^\circ$  on the position of 135mm because of the velocity value that was calculated 2.5m/s.

Although the balances of right and left regions are closest at the position of  $45^\circ$ , the highest values are seen at the position of  $90^\circ$ .

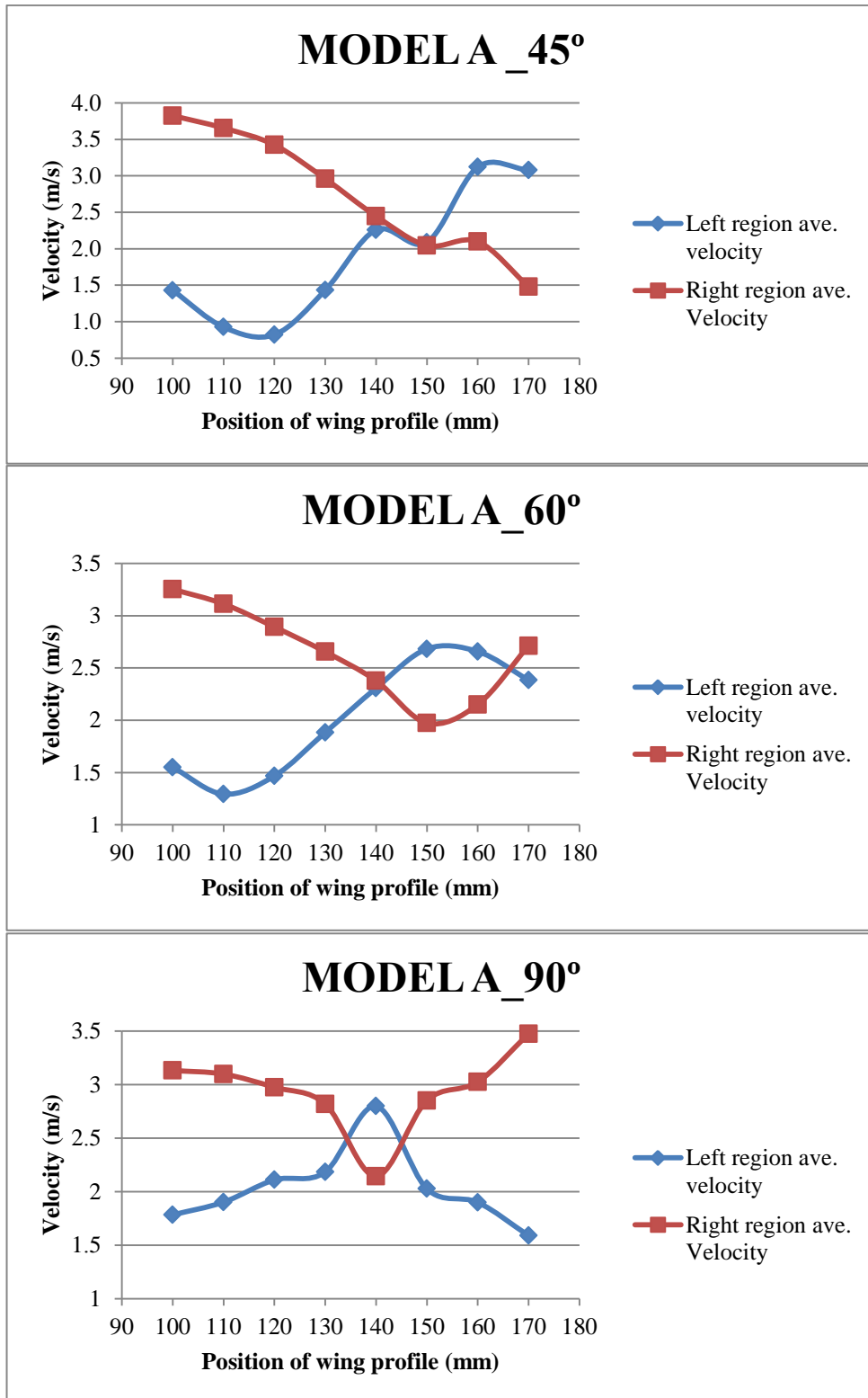


Figure 5.9 Model A parametric results.

Model B was designed appropriately to incline the flow direction to the left side throughout the duct. This baffle was carried out 10 different positions independent of angle parameter. Balance of average velocities was determined at the 130mm and 155mm positions where the curve charts are coincide with each other. If we compare the value of Model B at the balance positions, the values were also calculated less than Model A.

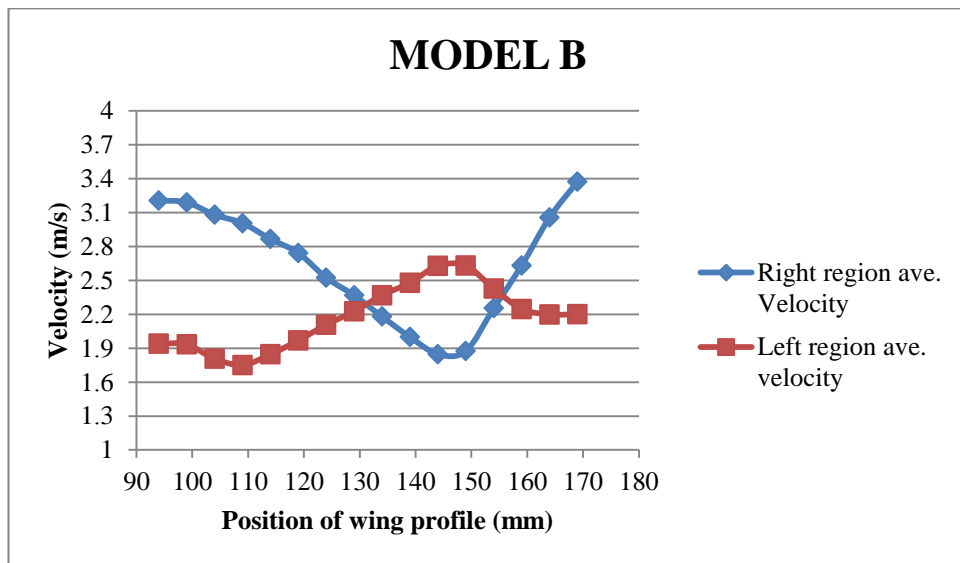


Figure 5.10 Model B parametric results.

Naca wing profiles were considered and friction was determined as priority during the Model C design process. Position of the baffle was also given a design parameter again.

Additionally three radius dimension was implemented for all positions throughout the duct to determine the effects of friction factor. The regions velocities' balance is converged with each other at 120mm position. Also average velocities of both side are increase the highest values at this position.

If we evaluate that outlet section has been divided as right and left region, result of investigation should be equalized average velocities as soon as possible and also highest values. Despite the fact that there isn't any position where the average velocities coincide with each other, highest velocity values were calculated Model C.

If three radius parameter of Model C is compared between the each other  $r=1.5\text{mm}$  condition has highest average velocity values at the position of 120mm.

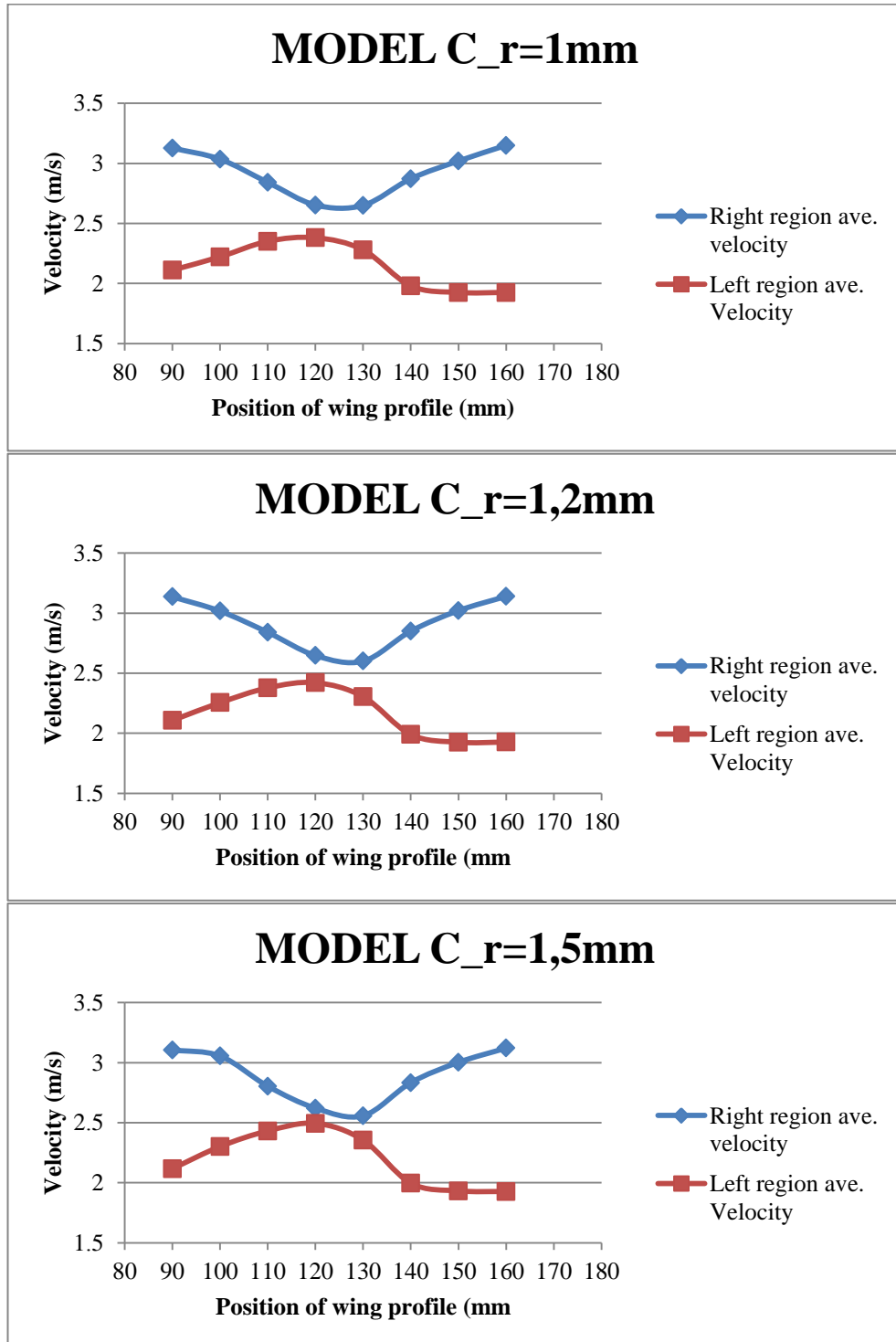


Figure 5.11 Model C parametric results.



## **CHAPTER SIX**

### **CONCLUSIONS**

The air flow at the exit region of the radial fan was investigated experimentally. It's also obvious that if we had implemented CFD analyses with a constant velocity value as the boundary condition, results couldn't have matched to the reality. Because of that reason PIV measurement method was chosen to determine the boundary conditions. Thus flow characteristics were resembled on the all control planes at the validation step.

It's useful to note that the unstable flow range of the fans' impellers was eliminated by means of successful implementation of PIV method. Boundary condition data was taken below the fan housing. This method prevented not only phenomena of the radial fan vorticities but also the uncertainty CFD results. Furthermore, convergence of the solutions was provided with lower mesh elements versus the all geometry that includes the radial fan.

Parametric investigations concerning different types and sizes of baffles inside the duct were conducted. Angle, radius, and position were determined the variables according to type of model. Both average velocity value and balance through the outlet of the duct were considered and Model C was determined at this conditions.

Utility of this study is developing a design method for radial fans behind the complexity of fan geometry by using a combination with a PIV set up as an experimental method and numerical study that includes different parameters. In conclusion that this combination method is provided to improvement design studies that are focused on some structures behind the fans faster and cheaper than the other methods.

## REFERENCES

- ASHRAE (American Society of Heating, Refrigerating and Air-Conditioning Engineers) (2006). *Refrigeration handbook*. Retrieved March 3, 2014, from [http://app.knovel.com/web/toc.v/cid:kpASHRAEH1/viewerType:toc/root\\_slug:ashrae-handbook-refrigeration/b-off-set:0/b-cat-id:219/b-off-set:0/b-order-by:name/b-sort-by:ascending/b-filter-by:all-content](http://app.knovel.com/web/toc.v/cid:kpASHRAEH1/viewerType:toc/root_slug:ashrae-handbook-refrigeration/b-off-set:0/b-cat-id:219/b-off-set:0/b-order-by:name/b-sort-by:ascending/b-filter-by:all-content).
- Capillary tube*, (n.d.). Retrieved February 9, 2014, from <http://www.cccme.org.cn/shop/chenxuecun/product---8.aspx>.
- Cengel, Y. A., & Boles, M. A. (2006). *Thermodynamics an engineering approach* (5th ed.). New York: McGraw Hill.
- Compact coiled air cooled condensing*, (n.d.). Retrieved February 8, 2014, from <http://vigilantinc.com/winecellars/images/cooling/ductlessSplit/whisperKOOL-mini-split-condenser>
- Condenser*, (n.d.). Retrieved February 11, 2014, from <http://www.ecplaza.net/product/static-condenser--179183-1433934.html>
- Cory, W.T.W. (2005). Fan history, types and characteristics. *Fans and Ventilation* (1<sup>st</sup> ed.), 22-26. Toronto: Elsevier Science.
- Cycle defrost evaporator*, (n.d.). Retrieved February 11, 2014, from <http://czxinxin.en.made-in-china.com/product/vbpnYuXwADWe/China-Tube-on-Plate-Evaporator.html>
- Dinçer, İ., & Kanoğlu, M. (2010). *Refrigeration systems and application* (2nd ed.). Chichester: Wiley.
- Eck, B. (1973). *Fans: Design and operation of centrifugal axial-flow and cross-flow*

- fans*.(1<sup>st</sup> ed.). (AZAD, R. & Scott, D. (Trans.). Oxford:Pergamon Press.
- Forced convection condenser*, (n.d.). Retrieved February 11, 2014, from [http://www.tradekorea.com/products/water\\_cooler\\_condenser.html](http://www.tradekorea.com/products/water_cooler_condenser.html).
- Frost free evaporator*, (n.d.). Retrieved February 11, 2014, from <http://trade.indiamart.com/details.mp?offer=1268063388>
- Heo, S. Cheong, C. & Kim, T. (2011). Development of low-noise centrifugal fans for a refrigerator using inclined S-shaped trailing edge. *International Journal of Refrigeration* (34), 2076-2091.
- ISO 15502 (International Organization for Standardization 15502) (2005). *Household refrigerating appliance-characteristic and test methods*.
- Jacob, R. Ray, S. Attridge, G. & Axford, N. (2000) *Manual of photography* (9<sup>th</sup> ed.), Oxford:Focal Press.
- Lee, S. Heo, S. & Cheong, C. (2010). Prediction and reduction of internal blade-passing frequency noise of the centrifugal fan in a refrigerator. *International Journal of Refrigeration*, 1129-1141.
- Özer, Ö. (2011). *Experimental investigations of velocity and temperature distribution inside a split air conditioners indoor unit*. Yüksek lisans tezi: Dokuz Eylül Üniversitesi. 98.
- Raffel, M., Willert, C., Werely, S. & Kompenhans, J. (2007). *Particle image velocimetry a practical guide* (2<sup>nd</sup> ed.). New York: Springer.
- Reciprocating compressor*, (n.d.). Retrieved February 10, 2014, from <http://www.scielo.br/img/revistas/jbsmse/v31n1>

*Refrigeraiton*, (n.d.) Retrieved December, 2010, from  
<http://en.wikipedia.org/wiki/Refrigerator>.

Yen, S. & Liu, J. (2007). Measurements of exit flow field of centrifugal fans with conditional sampling. *Journal of Marine Science Technology*. 232-240.